Acta Pharmaceutica Sinica B 2025;15(10):5346−5365

Chinese Pharmaceutical Association
Institute of Materia Medica, Chinese Academy of Medical Sciences

Acta Pharmaceutica Sinica B

www.elsevier.com/locate/apsb
www.sciencedirect.com

ORIGINAL ARTICLE

Discovery and proof-of-concept study of a novel highly selective sigma-1 receptor agonist for antipsychotic drug development

Wanyu Tang[a,†], Zhixue Ma[a,†], Bang Li[a,†], Zhexiang Yu[a,†], Xiaobao Zhao[a], Huicui Yang[a], Jian Hu[a], Sheng Tian[a,b], Linghan Gu[a], Jiaojiao Chen[a], Xing Zou[a], Qi Wang[a], Fan Chen[a], Guangying Li[a], Chaonan Zheng[a], Shuliu Gao[a], Wenjing Liu[a], Yue Li[a], Wenhua Zheng[c], Mingmei Wang[d], Na Ye[a,b,*], Xuechu Zhen[a,d,*]

[a]*Jiangsu Key Laboratory of Drug Discovery and Translational Research for Brain Diseases, College of Pharmaceutical Sciences, Soochow University, Suzhou 215123, China*
[b]*Jiangsu Province Engineering Research Center of Precision Diagnostics and Therapeutics Development, Soochow University, Suzhou 215123, China*
[c]*Center of Reproduction, Development and Aging, Institute of Translational Medicine, Faculty of Health Sciences, University of Macau, Macau SAR 999078, China*
[d]*College of Biology & Food Sciences, Suzhou University of Technology, Suzhou 215500, China*

Received 5 January 2025; received in revised form 28 February 2025; accepted 20 March 2025

KEY WORDS

Sigma-1 receptor;
Agonist;
Antipsychotic;
Central nervous system;
Schizophrenia;
Structure-based design;
Oxime ether;
Drug development

Abstract Sigma-1 receptor (σ_1R) has become a focus point of drug discovery for central nervous system (CNS) diseases. A series of novel 1-phenylethan-1-one *O*-(2-aminoethyl) oxime derivatives were synthesized. *In vitro* biological evaluation led to the identification of **1a**, **14a**, **15d** and **16d** as the most high-affinity ($K_i < 4$ nmol/L) and selective σ_1R agonists. Among these, **15d**, the most metabolically stable derivative exhibited high selectivity for σ_1R in relation to σ_2R and 52 other human targets. In addition to low CYP450 inhibition and induction, **15d** also exhibited high brain permeability and excellent oral bioavailability. Importantly, **15d** demonstrated effective antipsychotic potency, particularly for alleviating negative symptoms and improving cognitive impairment in experimental animal models, both of which are major challenges for schizophrenia treatment. Moreover, **15d** produced no significant extrapyramidal

*Corresponding authors.
E-mail addresses: yena@suda.edu.cn (Na Ye), zhenxuechu@suda.edu.cn (Xuechu Zhen).
[†]These authors made equal contributions to this work.
Peer review under the responsibility of Chinese Pharmaceutical Association and Institute of Materia Medica, Chinese Academy of Medical Sciences.

https://doi.org/10.1016/j.apsb.2025.04.028

symptoms, exhibiting superior pharmacological profiles in relation to current antipsychotic drugs. Mechanistically, **15d** inhibited GSK3β and enhanced prefrontal BDNF expression and excitatory synaptic transmission in pyramidal neurons. Collectively, these *in vivo* proof-of-concept findings provide substantial experimental evidence to demonstrate that modulating σ_1R represents a potential new therapeutic approach for schizophrenia. The novel chemical entity along with its favorable drug-like and pharmacological profile of **15d** renders it a promising candidate for treating schizophrenia.

1. Introduction

Schizophrenia is a severe psychiatric illness affecting approximately 1.1% of people worldwide[1,2]. There are three symptom domains for the disease: positive symptoms, negative symptoms and cognitive impairment. The currently available medicines for schizophrenia mainly target dopamine receptors by functioning as D_2 receptor antagonists/partial agonists with certain modulatory activity on other neurotransmitters, such as serotonin[3,4]. However, nearly 30% of patients do not respond to current antipsychotic treatment, and more than 50% of patients with schizophrenia suffer from relapse[4-6]. Hence, the development of novel antipsychotic drugs with novel targets and mechanisms of action is an unmet need for antipsychotic treatment.

Sigma-1 (σ_1R) is widely distributed in the central nervous system (CNS). Functionally, σ_1R acts as a Ca^{2+}-sensitive and ligand-operated receptor chaperone. Studies have revealed that σ_1R can undergo dynamic homo- and heteromerization in response to ligand binding, thereby regulating various biological functions[7-9]. Agonists generally stabilize the low molecular-weight form of σ_1R, whereas antagonists promote the formation of higher-order oligomers. Upon activation, σ_1R translocates to various organelles or plasma membranes and modulates a diverse array of targets, such as GPCR receptors (*e.g.*, D_1, D_2), ion channels (*e.g.*, NMDA, IP3, $Na_V1.5$), and signaling molecules (*e.g.*, Bip), to elicit wide regulatory effects on neuroplasticity and neurohemostasis[10-16]. Thus, σ_1R has been an actively pursued drug target for a variety of neurological and neuropsychiatric diseases. Numerous clinical and experimental evidence have also revealed the roles of σ_1R in schizophrenia[3,17-20]. For instance, the expression of σ_1R was found to be decreased in postmortem brains from schizophrenia patients[19,20], and several genetic studies have suggested an association between the σ_1R gene and schizophrenia[21]. Moreover, clinical studies have shown the beneficial effects of σ_1R activation in schizophrenia patients[22-24].

Currently, a diverse variety of small molecules targeting σ_1R have been developed and demonstrated to have therapeutic potentials in animal models of various CNS diseases. For schizophrenia, previous clinical trials and ongoing clinical studies have revealed the potentials of σ_1R agonists in schizophrenia treatment[3,10]. The systemic experimental evidence to reveal the therapeutic potentials of selective σ_1R agonists in schizophrenia, however, are not available. As a continuing effort to develop novel antipsychotic drugs[25-30], we herein reported the discovery of the potent and selective σ_1R agonist **15d** with a favorable drug-like profile, and provided the proof-of-concept *in vivo* experimental evidence of σ_1R agonists as promising antipsychotic agents.

2. Results

2.1. Structure-based design of σ_1R selective ligands

The majority of currently available σ_1R ligands were initially designed by employing Glennon's pharmacophore model for σ_1R[31-33], which incorporates two hydrophobic pharmacophores (P1 and P2) attached to a basic amine moiety, as shown in Fig. 1A. Recently, resolved cocrystal complexes of σ_1R bound with its ligands further expedite the development of new σ_1R ligands *via* structure-based drug design[34-36]. Developing novel candidates based on existing marketed drugs has emerged as an attractive and successful strategy to expedite the drug discovery process[37-40]. Given that many clinically used CNS-targeted drugs have moderate to high and promiscuous affinity toward σ_1R, they may offer an opportunity for repurposing existed chemical scaffolds to novel σ_1R selective ligands. Fluvoxamine is a potent and highly selective serotonin reuptake inhibitor (SSRI) with a K_i value of 2.2 nmol/L for serotonin transport (SERT)[41], but it also manifests moderate affinity toward σ_1R with a K_i value of 36 nmol/L[42,43]. Moreover, its characteristic oxime ether moiety is proposed to be a privileged scaffold in drug design and discovery[44-46], represented by siponimod, a selective sphingosine-1-phosphate receptor modulator approved for the treatment of multiple sclerosis[47], and the antiplatelet agent ridogrel[48]. Hence, we chose fluvoxamine as our starting point for the development of σ_1R selective agonists (Fig. 1B).

On the basis of the well-characterized co-crystal structure of a σ_1R agonist, **4-IBP**, in complex with human σ_1R (PDB ID: 5HK2)[35], we predicted that the nonselective σ_1R ligand fluvoxamine adopted an "h-style" binding mode to σ_1R *via* molecular docking studies (Fig. 2A). The terminal 4-trifluoromethylphenyl group of fluvoxamine, as a P1 fragment similar to the 4-iodophenyl moiety of **4-IBP**, extends into a hydrophobic pocket surrounded by key residues, including Met93, Leu95, Tyr103, and Leu105, while its methyoxybutyl and 2-aminoethyloxime side chains reach the other side of the binding pocket. The primary amino group of fluvoxamine also generates a salt bridge with Glu172. However, fluvoxamine actually lacks the classical P2 fragment despite the existence of its hydrophobic methoxybutyl moiety. Notably, this long hydrophobic ether tail also serves as a key pharmacophoric feature of typical SSRIs[49,50]. The X-ray cocrystal structure (PDB ID: 6AWP)[51] with engineered thermostable variants of the human serotonin transporter revealed that fluvoxamine adopted a "T-style" binding mode to SERT (Fig. 2B). We thus hypothesized that the 1-phenylethan-1-one *O*-(2-aminoethyl) oxime (PEOAEO) core of fluvoxamine obtained by removing the long hydrophobic ether tail would provide a basis for the discovery of novel highly potent and selective σ_1R ligands *via*

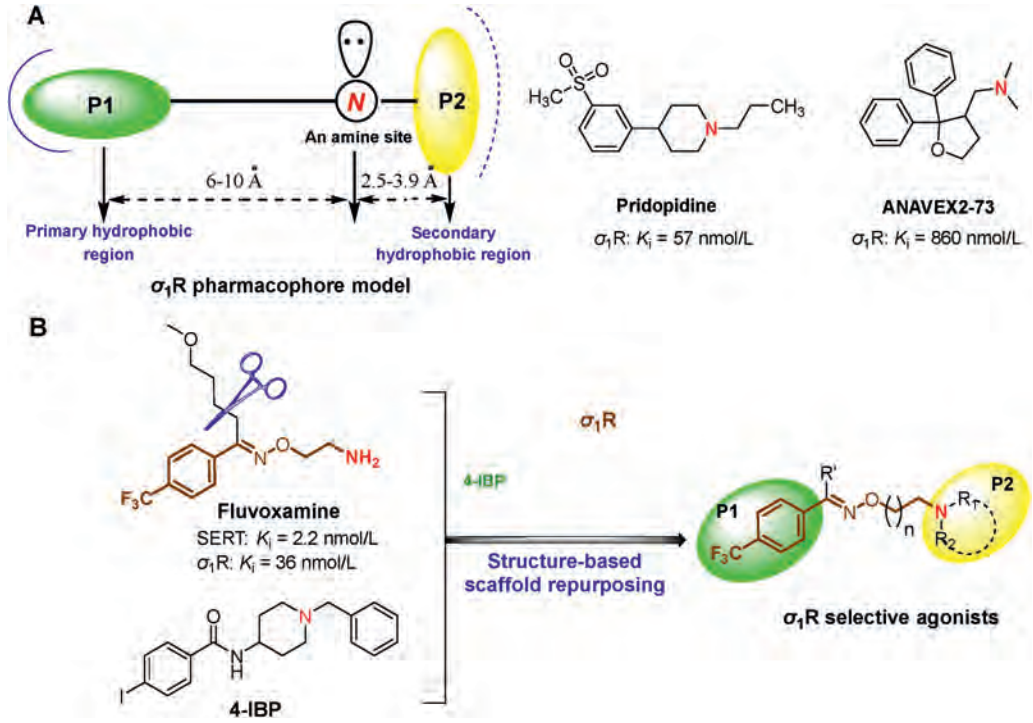

Figure 1 Structure-based design of σ_1R selective ligands. (A) σ_1R pharmacophore model and representative selective σ_1R agonists. (B) Design of our σ_1R selective ligands.

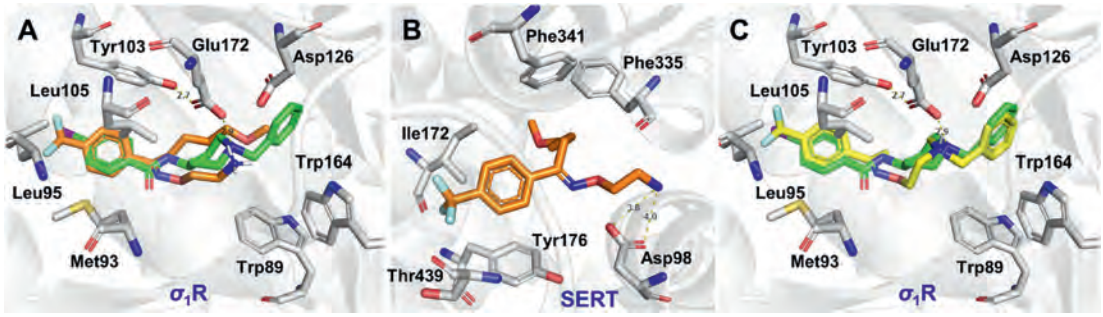

Figure 2 The molecular docking of fluvoxamine and designed σ_1R ligand **1a** with σ_1R. (A) Superposition of the nonselective σ_1R agonist fluvoxamine (brown stick model, docked binding pose) with **4-IBP** (green, PDB ID: 5HK2). (B) Interaction patterns between fluvoxamine and key residues in the binding site of the engineered thermostable variants of the human serotonin transporter (PDB ID: 6AWP). (C) Superposition of our designed σ_1R ligand **1a** (yellow stick model, docked binding pose) with **4-IBP** (green, PDB ID: 5HK2).

structure-based scaffold repurposing. Therefore, we carried out a medicinal chemistry optimization campaign by incorporating key P2 elements of σ_1R agonists into this skeleton. Our σ_1R ligand **1a** was first designed by attaching the P2 fragment of **4-IBP** to the primary amine of the PEOAEO core. As expected, **1a** adopts a highly similar linear binding mode to **4-IBP**, and the newly installed benzyl group extends to the other interior hydrophobic region of σ_1R surrounded by the residues Trp89, Asp 126, and Trp164 (Fig. 2C). In addition, compounds **2a**−**21a**, bearing diverse hydrophobic P2 moieties, were also designed to investigate their structure−affinity relationships (SAR), as shown in Table 1.

2.2. *Structure−affinity relationship (SAR) studies*

All the new compounds were synthesized (Supporting Information Schemes S1 and S2) and screened for their ability to inhibit the binding of [^{3}H]-(+)-pentazocine to σ_1R by using whole-brain homogenates from SD male rats in a radiolabeled binding assay[52]. As expected, the binding affinity of the reference, fluvoxamine, was identical to the reported value[41] (K_i 38 *vs* 36 nmol/L). We initially explored the effect of the substituents (R_1R_2) on the basic amine group (Table 1). By removal of the long ether chain and introduction of the aforementioned privileged *N*-methyl benzyl group (P2)[10], **1a** was found to exhibit 96-fold higher σ_1R affinity than fluvoxamine (K_i 0.44 *vs* 38 nmol/L), suggesting that this ether tail is not essential for binding to σ_1R as expected. However, removal of the *N*-methyl group of **1a** (as in **2a**) led to a significant loss of activity, and secondary aliphatic amines **3a** and **4a** also dramatically decreased the σ_1R affinity. The introduction of a small substituent (as in **5a**−**8a**) on the phenyl group of **1a** also led to a substantial decline in or even loss of σ_1R affinity. Only the 4-methoxyphenyl analog **6a** showed moderate σ_1R binding with a K_i value of 38.21 nmol/L. In addition,

Table 1 The discovery of PEOAEO-based derivatives as σ_1R ligands[a].

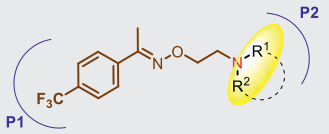

No.	NR_1R_2	σ_1R	
		Inhibition[a]	K_i (nmol/L)[b]
1a	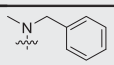	101.77%	0.44 ± 0.10
2a	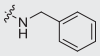	47.275%	–
3a		91.34%	182.6 ± 8.91
4a		77.71%	72.4%[c]
5a	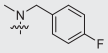	65.74%	–
6a	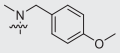	87.81%	38.21 ± 2.38
7a	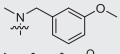	64.11%	–
8a	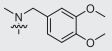	73.15%	50.93%[c]
9a		29.99%	–
10a		48.41%	–
11a		95.10%	48.30 ± 4.77
12a		96.03%	44.81 ± 3.54
13a		77.05%	49.53%[c]
14a		94.23%	0.63 ± 0.13
15a		53.87%	–
16a		45.94%	–
17a	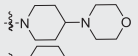	82.73%	136.05 ± 5.16
18a	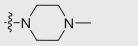	108.97%	55.16 ± 3.18
19a	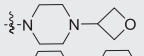	93.29%	107.7 ± 2.40
20a	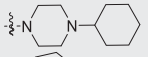	32.33%	–
21a		99.72%	156.75 ± 1.20
Fluvoxamine		81.76%	38 nmol/L (36 nmol/L[46])
(+)-Pentazocine		98.99%	3.29 nmol/L
Haloperidol		97.07%	1.87 nmol/L

[a]Values in % represent the inhibitory rate of radioligand binding at a test compound concentration of 10 μmol/L.

[b]When the inhibitory rate reached 75% at 1 μmol/L, the compound was subjected to further evaluation of its K_i value. The K_i values ± SEMs are the means of three independent experiments (n = 3).

[c]Values in % represent the inhibitory rate of radioligand binding at a test compound concentration of 1 μmol/L "–" indicates "not tested".

the cyclization of methyl and benzyl substituents at NR^1R^2 of **1a** resulted in a subseries of 5–7-membered cyclic amines **9a**–**11a**. Both isoindoline **9a** and tetrahydroisoquinoline **10a** completely lost activity, whereas tetrahydrobenzo[*c*]azepine **11a** and its isomer tetrahydrobenzo[*d*]azepine **12a** exhibited more than 100-fold decreased σ_1R affinities with comparable K_i values of 44.81–48.30 nmol/L. The bioisosteric replacement of tetrahydroisoquinoline **10a** with tetrahydro-[1,2,4]triazolo[4,3-*a*]pyrazine **13a** slightly increased the σ_1R affinity (inhibition at 10 μmol/L: 77.05% *vs* 48.41%). Notably, several cyclic amines have also been identified as privileged moieties for interaction with σ_1R[10,31]. Thus, removal of the fused phenyl ring of **9a** provided pyrrolidine **14a** with high σ_1R affinity (K_i = 0.63 nmol/L). Nevertheless, piperidine **15a** and morpholine **16a** still lack σ_1R activity, even though 4-(piperidin-4-yl)morpholine **17a** gains moderate σ_1R affinity (K_i = 136.05 nmol/L). Additionally, *N*-methyl piperazine **18a** and its analogs **19**–**20a** as well as azepane **21a** displayed moderate to low σ_1R affinities. These results reveal that the NR^1R^2 group in our PEOAEO scaffold is sensitive to structural modifications to interact with σ_1R, but tertiary amines, particularly the *N*-methyl benzyl group and pyrrolidine, may offer excellent σ_1R affinity.

As shown in Table 2, we then tuned the other two main pharmacophores of **1a** and **14a**, the substituted phenyl moiety (P1) and the alkyloxime linker, as in the *N*-methyl benzyl analogues **1b**–**h** and pyrrolidines **14b**–**d** and **14g**. Adjustment of the 4-trifluoromethyl group of **1a** and **14a** to either the 2- or 3-position (as in compounds **1b**–**c** or **14b**–**c**) resulted in a decrease in binding activity, suggesting that trifluoromethyl substitution at the 4-position of the phenyl group (P1) is beneficial to its binding activity. Moreover, extending the length (*n*) of their alkyloxime linkers also led to low σ_1R affinity, as in compounds **1d**–**1e** and **14d**. Additionally, replacement of the methyl group (R′) with either the smaller hydrogen atom (**1f**) or the larger trifluoromethyl (**1g**, **14g**) and phenyl groups (**1h**) all dramatically reduced the σ_1R affinity. Hence, **1a** and **14a** remain the most potent σ_1R ligands among these compounds.

Given the roles of other privileged P2 binding fragments, morpholine and piperidine moieties[10,53-56], were also chosen to establish a robust structure–affinity relationship, as shown in Table 2. In the piperidine series, both the 4- and 2-trifluoromethyl analogs **15a** and **15c** were inactive, whereas the 3-position analog **15b** resulted in a great increase in the σ_1R affinity, with a K_i value of 6.41 nmol/L. Moreover, inserting a methylene group into the linker of **15a** provided **15d** as the most potent analog in this series (K_i = 1.02 nmol/L), whereas elongation of the linker of **15b** resulted **15i** in decreased σ_1R affinity (K_i = 67.61 nmol/L). Furthermore, replacing the 4-trifluoromethyl group on the phenyl ring of **15d** with a more electron-withdrawing methylsulfonyl group (as in compound **15k**) resulted in a substantial reduction in σ_1R affinity (inhibition at 1 μmol/L: 70.32%). In contrast, introducing an electron-donating methoxy group (as in compound **15l**) resulted in a slight decrease in activity, with a K_i value of 39.44 nmol/L. Unfortunately, two methylene linker analogs of the morpholine series, **16a**–**c** and **16p**–**s**, regardless of the position or the kind of substituents on the phenyl ring, as well as the four-methylene linker analogs, **15e** and **16e**, all lost affinity for the receptor (inhibition at 1 μmol/L: ~76.88%). Nevertheless, the three-methylene linker analog of **16a**, **16d**, was the most potent σ_1R

ligand in this morpholine subseries, with a K_i value of 3.11 nmol/L; the 3-position analog of **15e** regained a moderate affinity, as in compound **15j** (K_i = 43.21 nmol/L). In addition, optimization of the methyl group (R′) by replacing it with a pheny ring (**15h**) or cyclizing it with the adjacent phenyl ring to form 5−6 membered rings (**15m**−**o**) resulted in decreased σ_1R affinity (K_i: 30.74−80.2 nmol/L), while substitution with a trifluoromethyl group (**15g** and **16g**) led to a significant loss of binding (inhibition at 10 μmol/L: 69.93%−76.30%). All these findings indicate that appropriate P1, P2, and linkage lengths are critical for ligand binding to σ_1R.

The above five high-affinity σ_1R ligands (K_i < 10 nmol/L) were then chosen to evaluate their selectivity over σ_2R. As expected, all of them exhibited high selectivity for σ_1R (39−948 folds, Table 3) over σ_2R, which is consistent with that of fluvoxamine (234-fold[57]).

Table 2 SAR study of PEOAEO-based derivatives.

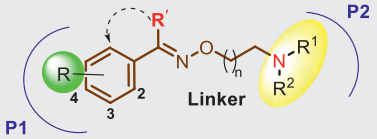

No.	R	R′	*n*	NR^1R^2	σ_1R	
					Inhibition[a]	K_i (nmol/L)[b]
1a	4-CF_3	Me	1		101.77%	0.44 ± 0.10
1b	3-CF_3	Me	1		67.89%	–
1c	2-CF_3	Me	1		72.33%	–
1d	4-CF_3	Me	2		100.34%	15.61 ± 1.40
1e	4-CF_3	Me	3		76.59%	51.28%[c]
1f	4-CF_3	H	1		105.43%	27.43 ± 0.86
1g	4-CF_3	CF_3	1		102.34%	33.74 ± 2.64
1h	4-CF_3	Ph	1		94.75%	67.40%[c]
14a	4-CF_3	Me	1		94.23%	0.63 ± 0.13
14b	3-CF_3	Me	1		56.39%	–
14c	2-CF_3	Me	1		85.85%	62.96%[c]
14d	4-CF_3	Me	2		93.98%	54.72%[c]
14g	4-CF_3	CF_3	1		67.43%	–
15a	4-CF_3	Me	1		53.87%	–
15b	3-CF_3	Me	1		103.63%	6.41 ± 1.80
15c	2-CF_3	Me	1		94.59%	73.56%[c]
15d	4-CF_3	Me	2		97.75%	1.02 ± 0.08
15e	4-CF_3	Me	3		91.57%	72.88%[c]
15g	4-CF_3	CF_3	2		76.30%	–
15h	4-CF_3	Ph	2		99.90%	56.09 ± 6.31
15i	3-CF_3	Me	2		97.30%	67.61 ± 6.23
15j	3-CF_3	Me	3		99.39%	43.21 ± 4.58
15k	4-$MeSO_2$	Me	2		91.26%	70.32%[c]
15l	4-OMe	Me	2		93.23%	39.44 ± 3.4
15m	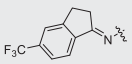		2		95.97%	30.74 ± 2.23
15n	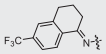		2		95.09%	86.20 ± 2.04
15o	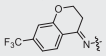		2		99.34%	76.25 ± 2.92
16a	4-CF_3	Me	1		45.94%	–
16b	3-CF_3	Me	1		86.67%	66.59%[c]
16c	2-CF_3	Me	1		94.83%	54.41%[c]
16d	4-CF_3	Me	2		99.17%	3.11 ± 0.01
16e	4-CF_3	Me	3		81.78%	57.8%[c]
16g	4-CF_3	CF_3	2		69.93%	–
16p	H	Me	1		74.41%	−8.25%[c]
16q	4-OMe	Me	1		93.16%	37.82%[c]
16r	4-Br	Me	1		105.52%	55.39%[c]
16s	4-Me	Me	1		66.17%	–

[a]Values in % represent the inhibitory rate of radioligand binding at a test compound concentration of 10 μmol/L.

[b]When the inhibitory rate reached 75% at 1 μmol/L, the compound was subjected to further evaluation of its K_i value. The K_i values ± SEMs are the means of three independent experiments (n = 3).

[c]Values in % represent the inhibitory rate of radioligand binding at a test compound concentration of 1 μmol/L "–" indicates "not tested".

Table 3 σ_1R and σ_2R binding affinities of potent PEOAEO-based derivatives.

No.	σ_1R K_i (nmol/L)[a]	σ_2R K_i (nmol/L)[a]	σ_1R selectivity[b]
1a	0.44 ± 0.10	134.6 ± 10.4	306
14a	0.63 ± 0.13	597.0 ± 86.6	948
15b	6.41 ± 1.80	249.8 ± 29.8	39
15d	1.02 ± 0.08	199.85 ± 31.65	196
16d	3.11 ± 0.01	1138.3 ± 159.75	366
(+)-Pentazocine	3.29 ± 0.90	672.6 ± 27.5	204
Haloperidol	1.87 ± 0.53	15.33 ± 3.27	8
DTG	35.55 ± 2.58	34.3 ± 7.65	1

[a]The data are expressed as the means ± SEMs from three independent experiments ($n = 3$).

[b]Ratios of the σ_2R K_i value to that of σ_1R for each compound were calculated.

We next employed a well-acceptable heterologous competition radioligand binding assay mediated by phenytoin (DPH)[56,58-60] to gain a general understanding of the functionality of the top 5 high-affinity σ_1R ligands ($K_i < 10$ nmol/L) which are more potent than all the clinically investigated σ_1R selective agonists (K_i 16−860 nmol/L) including pridopidine and ANAVEX2-73 (Fig. 1A)[10,11]. DPH, a low-potency positive allosteric σ_1R modulator, only increases the binding affinities of σ_1R agonists, whereas itself produces no effect or slightly decreases the binding of σ_1R antagonists. As shown in Table 4, *N*-methyl benzyl analogs **1a** (ratio: 5.90), pyrrolidine **14a** (9.12), piperidine **15d** (2.05), and morpholine **16d** (1.32), together with known σ_1R agonists PRE084 (1.98) and SKF10047 (7.10) in the presence of 250 μmol/L phenytoin, significantly shifted to increase the σ_1R binding affinity, with ratios of K_i without phenytoin/with phenytoin greater than 1, suggesting that they may act as σ_1R agonists. To our surprise, 3-trifluoromethyl analog **15b** (1.00) produces no effect on binding to σ_1R in the presence of 250 μmol/L phenytoin, and the known σ_1R antagonist BD1047 displayed slightly lower receptor binding affinity, with a ratio of K_i without phenytoin/with phenytoin of 0.64, indicating that **15b** may act as a σ_1R antagonist. These results indicate that the position of the substituent on the phenyl ring (P1) may reverse the function of the σ_1R ligands.

Table 4 Ratio of K_i values with or without phenytoin in the σ_1R radiolabeled binding assay[a].

No.	K_i (nmol/L)	K_i (nmol/L) + phenytoin	Ratios $K_i/(K_i$ + phenytoin)
1a	0.44 ± 0.10	0.07 ± 0.01	5.90 ± 0.80
14a	0.63 ± 0.13	0.07 ± 0.01	9.12 ± 0.46
15b	6.41 ± 1.80	6.32 ± 0.77	1.00 ± 0.16
15d	1.02 ± 0.08	0.51 ± 0.11	2.05 ± 0.30
16d	3.11 ± 0.01	2.39 ± 0.40	1.32 ± 0.23
PRE084	23.13 ± 3.17	12.43 ± 5.12	1.98 ± 0.56
SKF10047	292.31 ± 6.18	41.47 ± 5.20	7.10 ± 0.74
BD1047	0.87 ± 0.15	1.49 ± 0.71	0.63 ± 0.20

[a]Ratios of the K_i values for the compounds in the absence of DPH (control) to the K_i values obtained in the presence of DPH 250 μmol/L were tested and calculated as described in the Methods. The data are expressed as the means ± SEMs from three independent experiments ($n = 3$).

These four σ_1R selective agonists **1a**, **14a**, **15d** and **16d** were further evaluated for *in vitro* metabolic stability in rat and human liver microsomes. All of them were found to have approximately 3-fold greater metabolic stability in human liver microsomes (HLMs) than in mouse liver microsomes (MLMs). On account of the presence of methyl and benzyl substituents at NR^1R^2, the highest affinity σ_1R selective agonist **1a** ($K_i = 0.44$ nmol/L) rendered it more labile for metabolism in liver microsomes than cyclic amines **14a**, **15d** and **16d**. As shown in Supporting Information Table S1, acyclic amine **1a** exhibited a much shorter half-life and correspondingly higher clearance than the cyclic amines did in the decreasing order of piperidine **15d** > morpholine **16d** > pyrrolidine **14a**.

Notably, compound **15d** has the lowest clearance, with Cl_{int} values of 17.17 and 145.18 mL/min/mg in HLMs and MLMs, respectively (Table 5), along with the longest half-life, as evidenced by $T_{1/2}$ values of 101.27 and 37.59 min, respectively. Moreover, piperidine **15d** was also found to be stable in both human and mouse plasma ($T_{1/2} > 770$ min), with good plasma protein binding (~91%). In addition, fluvoxamine at 10 μmol/L significantly inhibited the enzymatic activity of CYP1A2 (95.74%) and CYP2C19 (95.02%) (Supporting Information Table S2), whereas compound **15d** did not significantly inhibit the five main CYP450 enzymes. Moreover, **15d** did not induce the enzymatic activity of CYP1A2 or CYP2D6 at 10.0 μmol/L. These results indicate the minimal risk of drug−drug interactions (DDIs) between **15d** and other drugs.

Hence, compound **15d** represents the most stable ($T_{1/2}$ 101.27 min in HLMs, 37.59 min in MLMs) putative σ_1R selective agonist with high-affinity ($K_i = 1.02$ nmol/L), which is therefore worthy of further investigation.

Table 5 *In vitro* drug-like properties of **15d**.

Parameter	Result
$T_{1/2}$ (H/M liver microsome)[a]	101.27/37.59 min
Cl_{int} (H/M liver microsome)[a]	17.17/145.18 mL/min/kg
$T_{1/2}$ (H/M plasma stability)	>770 min
Remaining (H/M plasma stability)[b]	99.1/98.4%
Plasma protein binding (H/M)[c]	91.1/90.6%
CYP1A2 inhibition[d]	3.45%
CYP2C9 inhibition[d]	−5.64%
CYP2C19 inhibition[d]	18.88%
CYP2D6 inhibition[d]	26.42%
CYP3A4 inhibition[d]	1.67%
CYP1A2 induction[e]	1.17-fold
CYP3A4 induction[e]	1.19-fold

[a]**15d** (1 μmol/L) was incubated with 0.5 mg/mL human or mouse liver microsomes for 45 min.

[b]The remaining percentage of **15d** (3 μmol/L) after incubation in human or mouse plasma for 120 min.

[c]The *in vitro* plasma protein binding of **15d** (5 μmol/L) was established using rapid equilibrium dialysis by shaking at 100 rpm for 6 h in human or mouse plasma.

[d]The inhibitory effect of **15d** (10 μmol/L) on CYP450 enzymatic activity was tested by using phenacetin (30 μmol/L), diclofenac (10 μmol/L), *S*-mephenytoin (35 μmol/L), bufuralol (10 μmol/L), midazolam (5 μmol/L), or testosterone (80 μmol/L) as CYP450 substrates.

[e]The effects of **15d** (10 μmol/L) on CYP450 enzymatic activity were tested by using omeprazole (50 μmol/L) and rifampicin (20 μmol/L) as CYP450 inducers.

2.3. *In vitro functional validation of compound **15d** on σ_1R*

σ_1R is known to associate with the binding immunoglobulin protein BiP (also called GRP78), which dissociates upon σ_1R activation. The measurement of the decreased binding between σ_1R and Bip is considered a reliable detection of receptor activation. As shown in Fig. 3A and B, compound **15d** dose-dependently induced σ_1R-Bip dissociation in HEK293T cells. Moreover, pharmacological activation of σ_1R is known to promote the phosphorylation of GSK3β-Ser9, subsequently leading to the inhibition of its enzymatic activity[61-63]. Thus, we assessed the effect of **15d** on the phosphorylation of GSK3β−Ser9 in HT-22 hippocampal neuronal cells (Supporting Information Fig. S1A and S1B). The cytotoxicity of **15d** was first tested, and it exhibited low cytotoxicity with an IC_{50} value of 95.44 ± 6.11 μmol/L in the MTT assay. The optimal concentration of compound **15d** on the phosphorylation of GSK3β-Ser9 was then assessed. The results presented in Fig. 3C and D demonstrated that all the tested concentrations (10 nmol/L, 100 nmol/L, 1 μmol/L and 10 μmol/L) of **15d** increased the phosphorylation of GSK3β-Ser9 under the current conditions, revealing that **15d** acts as a σ_1R agonist. **15d** at 1 μmol/L significantly enhanced the phosphorylation of GSK3β−Ser9 after up to 2 h of drug treatment, as shown in Fig. 3E and F, which is comparable with the widely used selective σ_1R agonist SKF10047[62]. Importantly, the phosphorylation of GSK3β induced by **15d** (1 μmol/L, 1 h) was blocked by the selective σ_1R antagonist BD1063 (Fig. 3G and H), further revealing the agonistic nature of **15d**. It was shown that σ_1R regulates the $[Ca^{2+}]_i$ increase evoked by store-operated Ca^{2+} entry (SOCE)[64-66]. To further confirm the agonistic activity of **15d**, we investigated the effect of **15d** on the SOCE-induced $[Ca^{2+}]_i$ increase in HEK-293 cells stably transfected with human σ_1R. Consistently, **15d** significantly inhibited the SOCE-induced $[Ca^{2+}]_i$ increase, similar to the effects of the σ_1R agonists SKF10047 and PRE084, whereas these effects were counteracted by the application of the selective σ_1R antagonists BD1063 or S1RA (Fig. 4). Taken together, these results further confirmed that compound **15d** is a σ_1R agonist.

2.4. *Selectivity profiles of compound **15d***

Preliminary radioligand binding assays (Supporting Information Table S3) revealed that **15d** at 10 μmol/L displayed no to weak binding (<47.9%) to dopamine receptors (D_1−D_5), 5-HT receptors (5-HT_{1A}R, 5-HT_{1B}R, 5-HT_{4E}R, 5-HT_{5A}R, 5-HT_6R, 5-HT_7R), dopamine transporters and norepinephrine transporters. Subsequently, a 44-panel early safety test was conducted based on both agonistic and antagonistic functional assays to reveal the selectivity of **15d**. As shown in Supporting Information Table S4, **15d** at 10 μmol/L resulted in weak or no activation or inhibition of a range of GPCRs, nuclear receptors, ion channels, enzymes, and transporters, except for 5-HT_{2A}, M_2, hERG and SERT (inhibition >50%). Notably, **15d** at 10 μmol/L showed no activation (−6.97%) and negligible inhibition (10.38%) for the 5-HT_{2B} receptor, which was reported to be associated with cardiac valvulopathy. Upon further analysis, **15d** was shown to act as a weak 5-HT_{2A} (IC_{50} = 1.62 μmol/L) receptor antagonist which may be beneficial for the treatment of schizophrenia. Moreover, it also functioned as a weak M_2 (IC_{50} = 1.06 μmol/L) receptor antagonist and exhibited low potency for hERG inhibition (IC_{50} = 2.45 μmol/L). To exclude the potential risk of cardiovascular effects associated with M_2 and hERG inhibition, a subsequent pharmacokinetic study was conducted in rhesus monkeys, in which electrocardiogram and blood pressure data were recorded simultaneously. The results revealed that compound **15d** had no cardiovascular side effects on this primate species (Supporting Information Table S5). Additionally, as expected, **15d** slightly inhibited the reuptake of serotonin, with an IC_{50} value of 5.65 μmol/L, which may be attributed to the lack of an essential pharmacophore featuring the methoxybutyl side-chain compared to the hit fluvoxamine (IC_{50} = 11.08 nmol/L). Overall, compound **15d** exhibited remarkable σ_1R selectivity (K_i = 1.02 nmol/L) against σ_2R (196-fold) and 52 other targets (>1000-fold) with a low risk of off-target effects.

2.5. *Molecular docking of compound **15b** and **15d** with σ_1R*

In addition to **15d**, we validated the functional activity of compound **15b**, which was previously identified as a putative σ_1R antagonist through DPH-mediated σ_1R radioligand binding assays. A rapid and sensitive NanoBiT assay to detect the interaction between σ_1R and Bip was recently reported[67]. We adopted this approach to evaluate the effects of **15b** and **15d** on the σ_1R and BiP associations. As shown in Supporting Information Fig. S2A, the interaction between σ_1R-LgBiT and BiP-SmBiT was enhanced after 16 h of treatment with compound **15b**, as evidenced by an increase in relative fluorescence, which mimicked the effect of the well-identified σ_1R antagonist BD1047, whereas treatment with the σ_1R agonist **15d** or PRE084 (Fig. S2B) decreased this interaction. Moreover, pretreatment with **15b** attenuated the agonist **15d** induced decrease in the interaction between σ_1R and Bip (Fig. S2C). These results provide reliable evidence supporting the antagonistic properties of compound **15b**.

Next, molecular docking studies based on the Glide XP scoring function were conducted to provide deep insights into the binding mechanisms of agonist **15d** and antagonist **15b** with σ_1R. As illustrated in Fig. 5A and Supporting Information Fig. S3, the docking poses of the highly selective σ_1R agonist **15d** and the σ_1R antagonist **15b** closely resemble those of the σ_1R agonist 4-IBP (PDB ID: 5HK2) and the σ_1R antagonists NE-100 (PDB ID: 6DK0) and haloperidol (PDB ID: 6DJZ) within the conservative orthosteric binding pocket of σ_1R. This binding pocket is defined by several dominant residues, including Met93, Leu95, Tyr103, Leu105, Phe107, Tyr120, Ile124, Asp126, Phe133, Val162, Glu172, Ile178, Thr202, and Tyr206 (Fig. 5B). A crucial salt bridge was formed between the nitrogen atoms of the piperidine rings in compounds **15b** and **15d** and residue Glu172 (Fig. 5C and D); however, their two piperidine rings adopted an almost perpendicular conformation relative to each other (Fig. 5A and B). Moreover, the 3-trifluoromethylphenyl group and the piperidine ring at both ends cause σ_1R antagonist **15b** to assume a U-shaped conformation (Fig. 5C), whereas the 4-trifluoromethylphenyl group and the piperidine ring lead σ_1R agonist **15d** to adopt a linear conformation (Fig. 5D). Furthermore, the 3-trifluoromethyl group of **15b** engages in hydrophobic interactions with residues Ile178 and Tyr103, whereas the 4-trifluoromethyl group of **15d** extends into a hydrophobic pocket formed by residues Thr202, Tyr206 and Leu95. Additionally, the piperidine ring of **15b** extends into a binding pocket formed by residues Tyr120, Ile124, and Asp126, while the piperidine ring of **15d** interacts

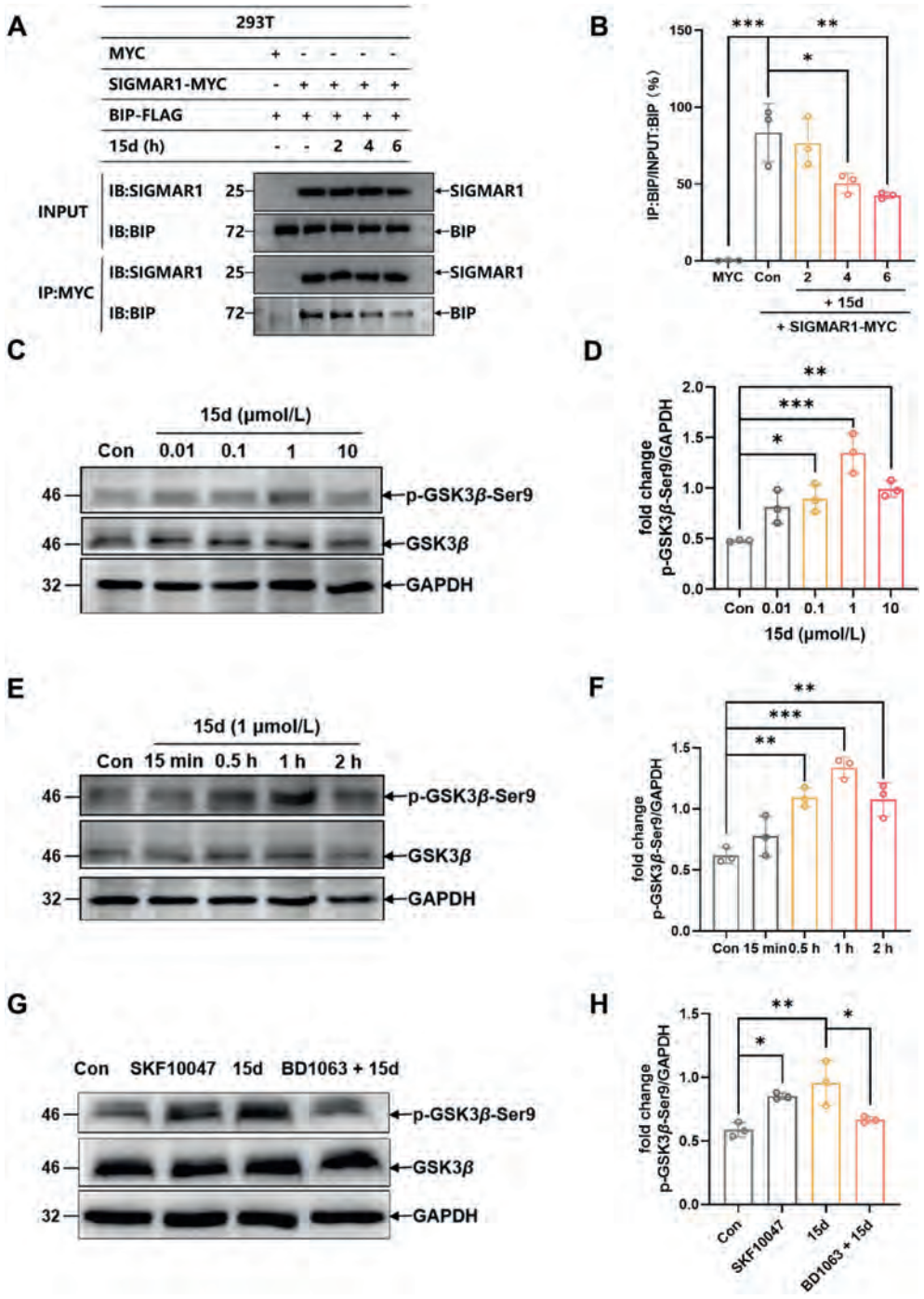

Figure 3 Effects of **15d** on σ_1R-Bip association and GSK3β-Ser9 phosphorylation. (A) HEK293T cells were co-transfected with BiP-FLAG along with MYC or SIGMAR1-MYC for 24 h. After stimulation of **15d** (10 μmol/L) for indicated time points, total cell lysates were immunoprecipitated using an anti-MYC antibody. The immunoprecipitates were detected by Western blot assay using an anti-FLAG antibody or anti-MYC receptor antibody. (B) Quantification of IP: BIP expression *via* image J software. (C) HT-22 cells were treated with vehicle or the corresponding concentration of **15d** (0.01, 0.1, 1 or 10 μmol/L) for 1 h before being harvested and lysed for Western blot analysis using respective antibody. (E) HT-22 cells were treated with 1 μmol/L compound **15d** at 15 min, 0.5, 1 and 2 h, respectively, before being collected for Western blot analysis. Representative images showing the expression of *p*-GSK3β-Ser9 and GSK3β *via* respective anti-rabbit (1:1000) or anti-mouse (1:1000) antibodies. (G) HT-22 cells were pretreated with the selective σ_1R antagonist BD1063 (1 μmol/L) for 0.5 h prior to and during treatment with 1 μmol/L **15d** for an additional 1 h before being harvested for Western blot analysis. The selective σ_1R agonist SKF10047 (1 μmol/L, 1 h) was used as a positive control. (C, F, H) Quantitative data of the expression of p-GSK3β-Ser9 *via* image J software. All the experiments were carried out 3 times independently. The data are presented as the mean ± SD, $n = 3$. Statistical analysis was performed *via* one-way ANOVA followed by Tukey's multiple comparisons test was used. $^*P < 0.05$, $^{**}P < 0.01$, $^{***}P < 0.001$.

hydrophobically with residues Phe133 and Val162. These findings could offer some helpful tips for finding new σ_1R agonists or antagonists in the future. The cryo-EM structure of **15d** in complex with σ_1R is currently being resolved and will be reported in a separate publication.

2.6. *Pharmacokinetics (PK) and brain penetration of compound **15d***

Encouraged by favorable metabolic and selective profiles, the PK of **15d** was subsequently assessed in C57BL/6J mice following a single intravenous administration at a dose of 5 mg/kg or oral administration at a dose of 10 mg/kg. Although the clog*P* value of **15d** is calculated as 4.28 (https://molinspiration.com/cgi/properties), its hydrochloride salt (**15d**·HCl) exhibits a remarkable aqueous solubility of 220 mg/mL in brine. Compound **15d**·HCl was unambiguously identified as an (*E*)-geometrical isomer *via* X-ray analysis (Table 6). Consequently, **15d**·HCl is used for *in vivo* PK studies. Compound **15d** presented a decent half-life ($T_{1/2}$), rapid time to achieve maximum concentration (T_{max}), moderate plasma clearance (CL), and extensive volume of distribution in plasma (V_{ss}), as summarized in Table 5. Additionally, compound **15d** exhibited a low maximum serum concentration (C_{max}) of 200−279 ng/mL and moderate plasma exposure ($AUC_{0-\infty}$) of 789−1206 ng h/mL, indicating low likelihood of inducing peripheral side effects. Notably, an excellent oral bioavailability (*F*) of 76.4% was observed. We also assessed blood−brain barrier (BBB) permeability of **15d** following oral administration at a dosage of 10 mg/kg. As shown in Table 5 and Supporting Information Table S6, the total brain-to-plasma concentration ratios (B/P) of **15d** were 34.7−46.1 and 18.3−30.1 at 0.5 and 4 h, respectively. The brain concentration reached 9730 and 8580 ng/g at 0.5 h following single 5 mg/kg intravenous administration and single 10 mg/kg oral administration, respectively (Table S6), indicating excellent BBB permeability of **15d**. All these results demonstrated the outstanding PK profile of **15d** to support its *in vivo* efficacy.

2.7. *Compound **15d** dose-dependently reduces PCP-induced hyperlocomotion and prepulses inhibition deficits*

To explore the potential of **15d** in the treatment of schizophrenia, we first assessed the effects of **15d** on phencyclidine (PCP)-induced hyperactivity and prepulse inhibition (PPI) deficits in mice, in comparison with the atypical antipsychotic drug risperidone (1 mg/kg)[68,69]. As shown in Fig. 6A, **15d** significantly attenuated PCP-induced hyperlocomotion in a dose-dependent manner, as did in PPI (Fig. 6A and E). Similarly, the σ_1R selective agonist SA4503 also significantly reduced PCP-induced hyperactivity at a dose of 30 mg/kg (Fig. 6B). Notably, fluvoxamine administration, up to 90 mg/kg (Fig. 6A), failed to induce the same effects as **15d** did, which is consistent with its nonselective agonistic activity on σ_1R and is also in agreement with the poor efficacy of the drug on positive symptoms in schizophrenia patients[70-73].

Moreover, the effects of **15d** on PCP-induced hyperlocomotion and PPI deficits were blocked by pretreatment with the selective σ_1R antagonist BD1063, indicating a σ_1R-mediated event (Fig. 6C, D and F). In support of these findings, the effects of **15d** on the disruption of PPIand hyperactivity in response to PCP disappeared in σ_1R knockout mice (Fig. 6G and H).

2.8. *Compound **15d** improves social deficits and spatial working memory impairment*

We next assessed the effects of **15d** on chronic PCP-induced impairments in social interaction (SI) and novel object recognition (NOR), the two classic assessments for negative symptoms and cognitive impairment, respectively, both of which are widely used in schizophrenia drug evaluation. We employed 7.5 mg/kg dose of PCP, which we found reproducibly induced the expected damage to working memory and social interaction, as previously reported[28]. As shown in Fig. 7A, the total social interaction time (SI) in PCP-treated mice was significantly lower than that in control mice, whereas **15d** treatment for 1 week dose-dependently increased the SI time in PCP-treated mice. Moreover, **15d** also ameliorated chronic PCP-induced impairment in the NOR test in terms of both exploration time (Fig. 7B) and the discrimination index (Fig. 7C). Moreover, the application of the selective σ_1R antagonist BD1063 (30 mg/kg, ip) blocked the effects of **15d** (30 mg/kg, *po*) -ameliorated impairment in both the SI (Fig. 7D) and NOR induced by PCP (Fig. 7E and F). Increased levels of phosphorylation at GSK3β-Ser9 and elevated BDNF expression were also observed *in vivo* (Fig. S1C−S1F). These results indicate that **15d** significantly ameliorates impairments in both cognition and SI induced by chronic PCP, which is dependent on the σ_1 receptor, presumably *via* promoting BDNF production.

2.9. *Compound **15d** administration induces no cataleptic effects within the antipsychotic dose range*

One major adverse effect of current antipsychotic drugs is their extrapyramidal effects. We next determined whether **15d** elicited anti-psychotic effect at the cost of cataleptic response in the catalepsy bar test. As shown in Fig. 9, no significant cataleptic responses were observed in any of the groups receiving doses ranging from 10 to 45 mg/kg **15d**. In contrast, catalepsy induced by 3 mg/kg risperidone was observed (Fig. 8). The peak response effect of 3 mg/kg risperidone was observed at 60 min post-administration, with a mean catalepsy duration of 49.57 min. Collectively, these findings demonstrate that the selective σ_1R agonist **15d** elicits no extrapyramidal effect at therapeutic doses.

2.10. *Compound **15d** promotes excitatory synaptic transmission of S1BF L2/3 pyramidal neurons in a σ_1R-dependent manner*

In agreement with our previous report[28], basal synaptic transmission was not significantly changed in σ_1R knockout mice in relation to wide type mice. To elucidate the role of σ_1R activation in **15d**-induced effects, we employed cortical brain slices to examine the effect of **15d** on synaptic transmission in adult P14 mice *via* electrophysiological experiments. After acute brain slices were perfused with **15d** (1 μmol/L), the frequency of spontaneous excitatory postsynaptic currents (sEPSCs) and the amplitude of L2/3 pyramidal neurons in the barrel field of the primary somatosensory cortex (S1BF) significantly increased within minutes (Fig. 9A and B). However, the increase in excitatory synaptic transmission was eliminated in the σ_1R knockout mice (Fig. 9E and F). Additionally, inhibitory synaptic transmission, as

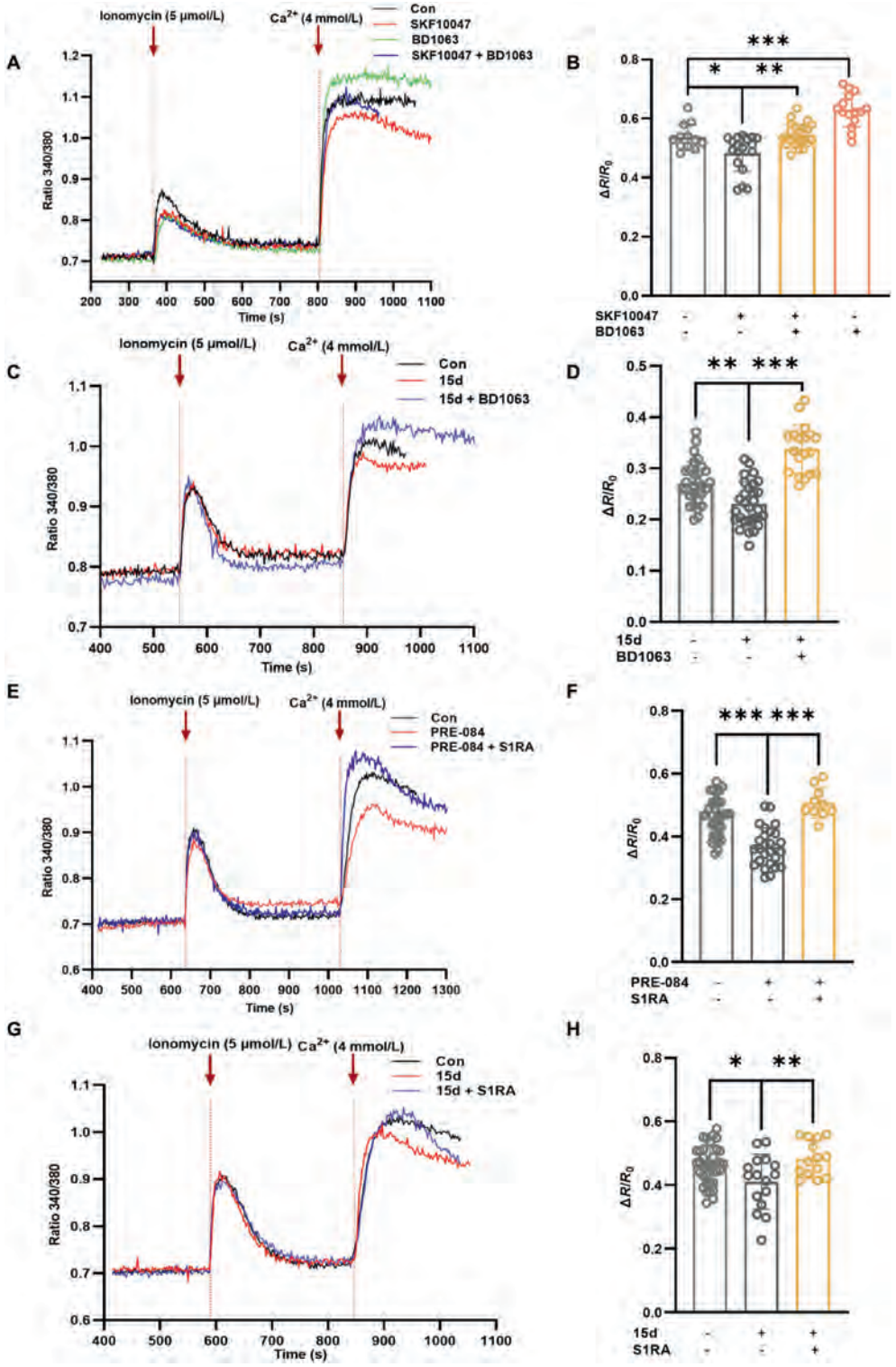

Figure 4 Effects of **15d** on the SOCE-induced $[Ca^{2+}]_i$ increased in HEK-293 cells stably expressing σ_1R. (A−D) HEK-293 cells stably expressing σ_1R were pretreated with different ligands (5 μmol/L SKF10047, 10 μmol/L BD1063 or 5 μmol/L SKF10047 + 10 μmol/L BD1063 for A and B; 10 μmol/L **15d** or 10 μmol/L **15d** + 10 μmol/L BD1063 for C and D) in Ca^{2+}-free HBSS before the addition of 5 μmol/L ionomycin and subsequent restoration of extracellular Ca^{2+} ($CaCl_2$ 4 mmol/L). (E−H) HEK-293 cells were pretreated with different ligands (25 μmol/L PRE-084, 100 μmol/L S1RA or 25 μmol/L PRE-084 + 100 μmol/L S1RA for E and F; 10 μmol/L **15d** or 10 μmol/L **15d** + 100 μmol/L S1RA for G and H) in Ca^{2+}-free HBSS before the addition of 5 μmol/L ionomycin and subsequent restoration of extracellular Ca^{2+} ($CaCl_2$ 4 mmol/L). Ca^{2+} signals, reflected by the fluorescence ratio F_{340}/F_{380}, were recorded from populations of Fura-2AM loaded HEK-293 cells. The results (A, C, E and G) show the mean responses from at least six replicates. The summary results (B, D, F and H) show peak increases in $[Ca^{2+}]_i$ after the restoration of extracellular Ca^{2+} to ionomycin-treated HEK cells. All summary results are presented as the mean ± SD. $n = 12-37$. $^*P < 0.05$, $^{**}P < 0.01$, $^{***}P < 0.001$. ANOVA with Tukey's *post-hoc* analysis was used (C, D, G and H).

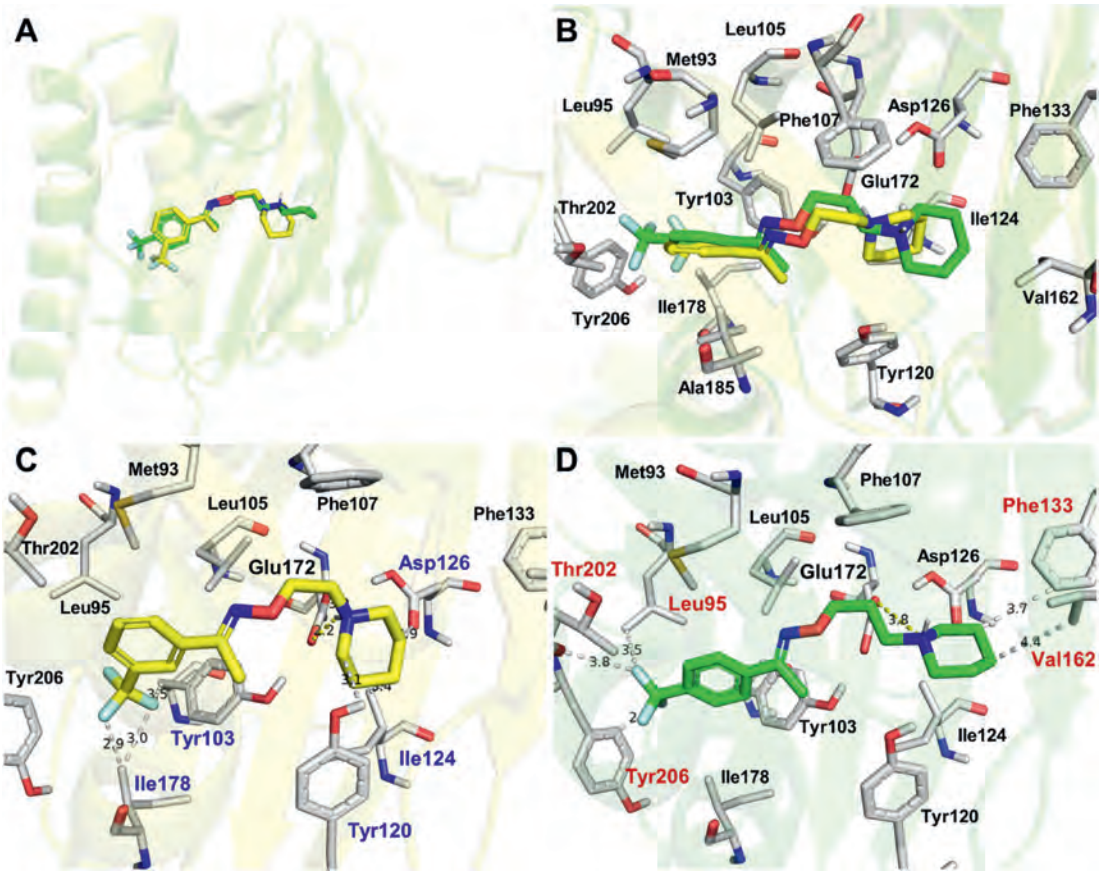

Figure 5 The molecular docking of **15b** and **15d** with σ_1R. (A) Overlay of the predicted docking poses of **15b** (yellow, PDB ID: 5HK2) and **15d** (green, PDB ID: 6DK0) in the binding pocket of σ_1R. (B) The σ_1R binding pockets of compounds **15b** (depicted in yellow sticks) and **15d** (depicted in green sticks). (C) Predicted docking pose of **15b** in the binding pocket of the inactive σ_1R (PDB ID: 6DK0). The amino acids within 4 Å of the 3-trifluoromethyl and piperidine groups are highlighted in blue. (D) Predicted docking pose of **15d** in the binding pocket of the active σ_1R (PDB ID: 5HK2). The amino acids within about 4 Å of the 4-trifluoromethyl and piperidine groups are highlighted in dark red.

indicated by the frequency and amplitude of spontaneous inhibitory postsynaptic currents (sIPSCs), was not significantly affected by **15d** perfusion (Fig. 9C, D, G, and H). Taken together, it appears that **15d** promotes excitatory synaptic transmission in the S1BF L2/3 pyramidal neurons of P14 mice in a σ_1R-dependent manner, while inhibitory synaptic transmission was not significantly altered.

*2.11. Toxicology safety evaluation of **15d** in mice*

In addition to its low off-target potentials, compound **15d** was also found to be negative in the mini-AMES test against Salmonella typhimurium strains TA98 and TA100. Moreover, we also predicted the phospholipidosis potential of compound **15d** since cationic amphiphilic drugs may induce phospholipidosis[74]. The

Table 6 X-ray crystal structure and *in vivo* pharmacokinetic profile of **15d** in C57BL/6 mice[a].

X-ray crystal structure[b]	Dose (mg/kg)	5 mg/kg, iv	10 mg/kg, *po*
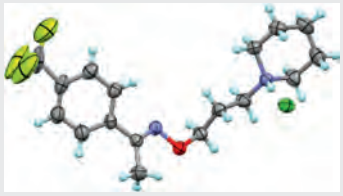	T_{max} (h)	0.08 ± 0	0.75 ± 0.43
	C_{max} (ng/mL)	279 ± 4.51	200 ± 7.09
	$AUC_{0-\infty}$ (ng/h/mL)	789 ± 139	1206 ± 351
	$T_{1/2}$ (h)	4.52 ± 0.87	4.27 ± 0.67
	CL (L/h/kg)	6.46 ± 1.07	/
	V_{ss} (L/kg)	42.22 ± 11.12	/
	F (%)	/	76.4 ± 0.22
	B/P ratio[c]	34.7 (0.5 h)	46.1 (0.5 h)
		18.3 (4 h)	30.1 (4 h)

[a]Values are the average of three runs. Compound **15d**·HCl was dissolved in saline and administrated by intravenous (iv) or oral gavage (*po*). Plasma samples were collected and tested to calculate the PK parameters.
[b]The X-ray crystal structure of **15d**·HCl.
[c]Ratio of the concentration of **15d** in brain tissue to the value in plasma was calculated as the B/P ratio. "/" means "not determined".

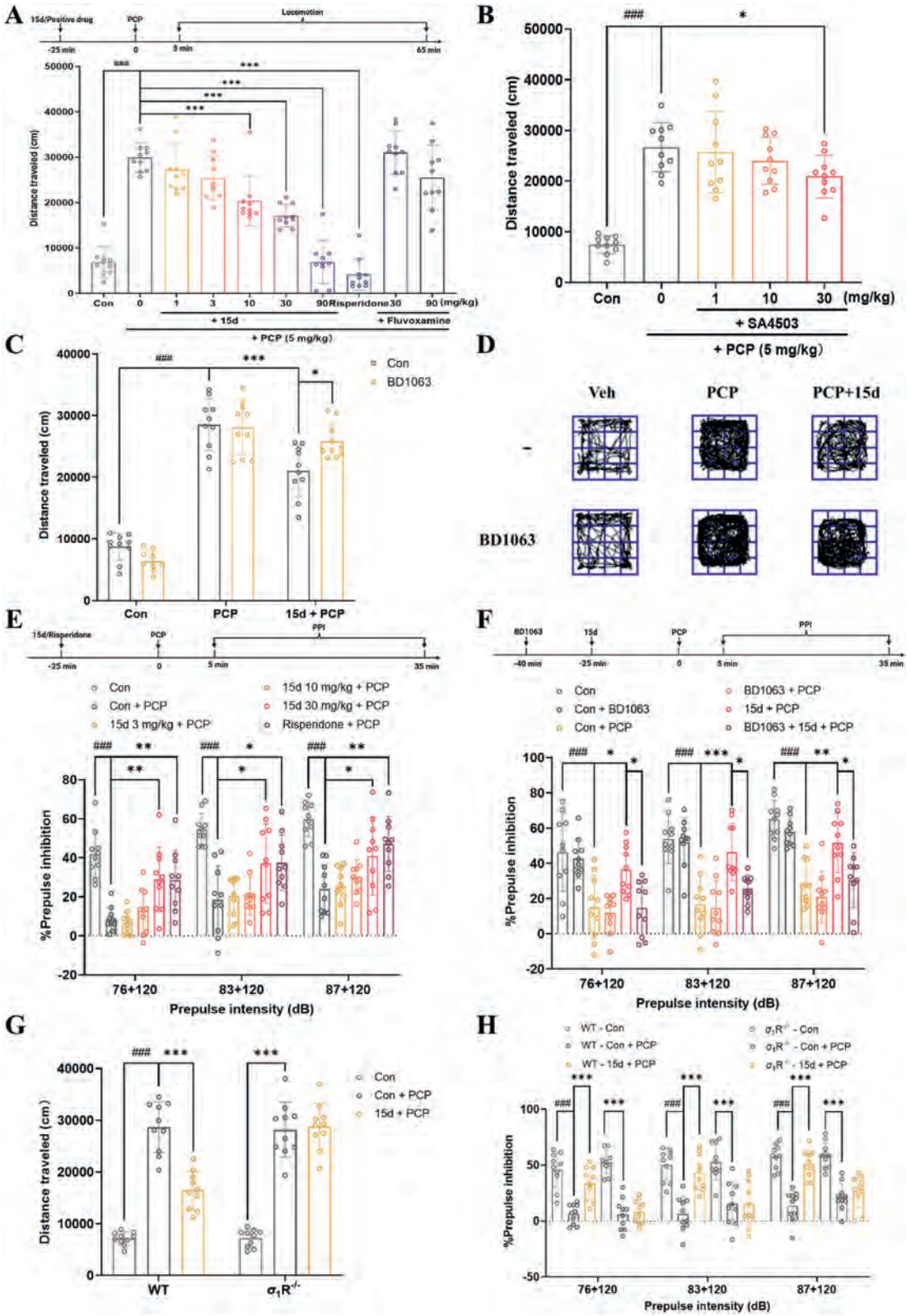

Figure 6 Oral administration of **15d** dose-dependently reduced PCP-induced hyperlocomotion activity and PPI defects *via* σ_1R in C57BL/6 mice. (A) A single subcutaneous injection of 5 mg/kg PCP induced hyperactivity in C57BL/6 mice. **15d**·HCl (1, 3, 10, 30 and 90 mg/kg), risperidone (1 mg/kg) or fluvoxamine (30 and 90 mg/kg) was administered orally 25 min before PCP administration. Locomotor activity was recorded over a 60 min period. The statistical chart of distance within 60 min is shown above. (B) SA4503 (1, 10, or 30 mg/kg) was administered orally 25 min before PCP administration. Locomotor activity was recorded over a 60 min period. A summary bar graph of the distance traveled is shown. (C, D) The σ_1R selective antagonist BD1063 blocks the **15d**-ameliorated hyperactivity induced by PCP. The mice were intraperitoneally

recently developed machine learning platform AMALPHI[75] indicates that **15d** has 67.14% of probability as a phospholipidosis inducer. However, compound **15d** exhibited low antiviral activity (IC_{50}: 133.4−396.4 μmol/L) against SARS-COV-2, Zika virus, and yellow fever virus. Based on the highly significant positive correlations between the ability of cationic amphiphilic drugs to induce phospholipidosis and their antiviral activity[76], it may imply that **15d** actually has a low probability to provoke phospholipidosis. Furthermore, ICR mice were subjected to 7-day dose-range finding (DRF) toxicology studies for **15d**, and we found that mice were well tolerant to either single dose (50, 100, or 150 mg/kg/day) or twice a day (50, 75, or 100 mg/kg/day) *via* oral treatment for a week. Transient convulsions, tachypnea and decreased movement were observed in some animals on Days 2−5 during dosing, but they recovered within 1−2 h, indicating that compound **15d** is rapidly metabolized and that such pharmacological responses are reversible. As summarized in Supporting Information Table S7, there was a correlation between systemic exposure and dosage after Day 1 administration of **15d**. Continuous administration for 7 days resulted in a decrease in plasma exposure compared to the initial dose, indicating a low likelihood of cumulative toxicity. Furthermore, the concentration of compound **15d** in the target organ exhibited a descending order as follows: liver > kidney > brain > heart, and no body weight loss was observed (Supporting Information Fig. S7). The low concentration of **15d** in the cardiac tissue may also contribute to its weak cardiac effects.

3. Discussions

Since the discovery of the first antipsychotic drug chlorpromazine in the 1950s, D_2 dopamine receptor based antipsychotic drugs have dominated for decades[5,77-80]. These drugs effectively relieve positive symptoms; however, they have limited efficacy against negative symptoms and cognitive function. The disadvantages of dopamine receptor-based antipsychotic drugs include target-related unwanted effects such as EPS and metabolic problems. Although tremendous efforts have been made to identify new targets (*e.g.*, M_4, PDE10A, DAAO, GlyT1, TAAR, and GPR139) and new mechanisms for schizophrenia treatment[3], only limited drugs with different mechanisms have been delivered to clinical use so far. σ_1R has become a focus point in CNS drug discovery because of its important regulatory roles in neuroplasticity, neuroimmune/inflammation, neuroprotection and repair[10,14,16]. The potent effects of σ_1R modulators on cognitive function and memory have been firmly demonstrated both in experimental and clinical studies[10,63,81]. With respect to antipsychotic effects, several previous clinical trials of drugs possessing σ_1R agonistic activity have shown beneficial effects in schizophrenia patients[70,82,83]. We previously reported that the application of allosteric modulation of σ_1R elicited excellent efficacy in relieving negative symptoms and improving cognitive function in schizophrenia-like animal models[28]. However, the potential therapeutic effects of selective σ_1R agonists in schizophrenia have never been evaluated systemically.

In the present study, a series of novel PEOAEO derivatives were synthesized by using the scaffold of the existing SERT inhibitor fluvoxamine (SERT IC_{50} = 11.08 nmol/L; σ_1R K_i = 38 nmol/L). We identified **15d** as a σ_1R selective agonist (σ_1R K_i = 1.02 nmol/L; SERT IC_{50} = 5652 nmol/L). Scaffold repurposing, as a valuable complement to drug repurposing, has emerged as an attractive strategy to accelerate the drug discovery process, which not only preserves the exceptional properties of the original parent framework but also effectively addresses various challenges associated with drug repurposing, such as limited efficacy and narrow intellectual property space[39,40,84,85]. Despite the inclusion of four σ_1R selective agonists in clinical trials, SA4503 and T-817MA have been discontinued, whereas pridopidine and ANAVEX2-73 (blacamesine), the remaining two clinically active σ_1R agonists, demonstrate moderate affinity for σ_1R (K_i = 57 & 860 nmol/L, respectively)[86]. Their σ_1R selectivity, however, is relatively modest (3.8−28.6 folds) because they also have certain affinities for dopamine D_3 (K_i = 1630 nmol/L) and muscarinic receptors (K_i = 3300−5200 nmol/L)[31]. However, PET studies of pridopidine conducted in both healthy volunteers and Huntington disease patients revealed that it exhibited ∼90% σ_1R occupancy and only ∼3% D_2/D_3 receptor occupancy[87]. And ANAVEX2-73 has submitted a marketing authorization application to the European Medicines Agency (EMA) on Nov 26, 2024, for the treatment of Alzheimer's disease, in which the modulation of σ_1R activity is believed to be the major contributor to its efficacy. Although efforts have been made to identify highly selective σ_1R agonists with favorable drug-like properties[10,31], there is few candidate processed to clinical study, most likely attributing to their disadvantage in drug-like properties. The recently discovered selective σ_1R agonist 14qR exhibited good selectivity (WLB-87848: σ_1R K_i = 9 nmol/L; σ_2R K_i > 1000 nmol/L) and fair BBB permeability (B/P: 0.95) but had a relatively short half-life ($T_{1/2}$: 0.9 h)[88]. The presently discovered σ_1R selective agonist **15d**

injected with 30 mg/kg BD1063 15 min before **15d**·HCl treatment. 25 min after oral administration of 30 mg/kg **15d**·HCl, saline or 5 mg/kg PCP was subcutaneously injected. (C) Representative tracks of the mice in the first 5 min. (D) Locomotor activity was then measured 5 min after PCP injection. The statistical chart of distance within 60 min is shown above. (E) Oral administration of **15d** restored the PPI. A single subcutaneous injection of 5 mg/kg PCP induced PPI damage in mice. **15d**·HCl (3, 10 or 30 mg/kg) or risperidone (1 mg/kg) was administered orally 25 min, before PCP administration. PPIs at three different prepulse intensity levels were measured (76, 83 and 87 dB) 5 min after PCP administration. (F) The σ_1R selective antagonist BD1063 attenuated the **15d**-ameliorated PPI disruption. Mice were intraperitoneally injected with 30 mg/kg BD1063 15 min before oral administration of 30 mg/kg **15d**·HCl. 25 min after treatment with **15d**·HCl, saline or 5 mg/kg PCP was subcutaneously injected. The PPI test was subsequently measured 5 min after PCP injection. PPIs at three different prepulse intensity levels were measured (76, 83 and 87 dB). (G) Treatment with **15d** failed to improve PCP-induced hyperlocomotion activity in σ_1R knockout mice. **15d**·HCl (30 mg/kg) was administered orally 25 min before PCP administration. Locomotor activity was recorded over a 60 min period. A summary bar graph of the distance traveled is shown. (H) Treatment with **15d** failed to improve prepulse inhibition (PPI) deficiency induced by acute PCP administration in σ_1R knockout mice[28]. A single subcutaneous injection of 5 mg/kg PCP induced PPI damage in both wild-type and $\sigma_1R^{-/-}$ mice. **15d**·HCl (30 mg/kg) was administered orally 25 min before PCP administration. PPIs at three different prepulse intensity levels were measured (76, 83 and 87 dB) 5 min after PCP administration. Data are shown as the mean ± SD; n = 10 mice per group. Statistical analysis was performed *via* one-way ANOVA (A, B) and two-way ANOVA (C, E, F, G and H); $^*P < 0.05$, $^{**}P < 0.01$, $^{***}P < 0.001$ compared to Con + PCP. $^{\#\#\#}P < 0.001$ compared to Con. Data are presented as mean ± SEM are provided in Supporting Information Fig. S4.

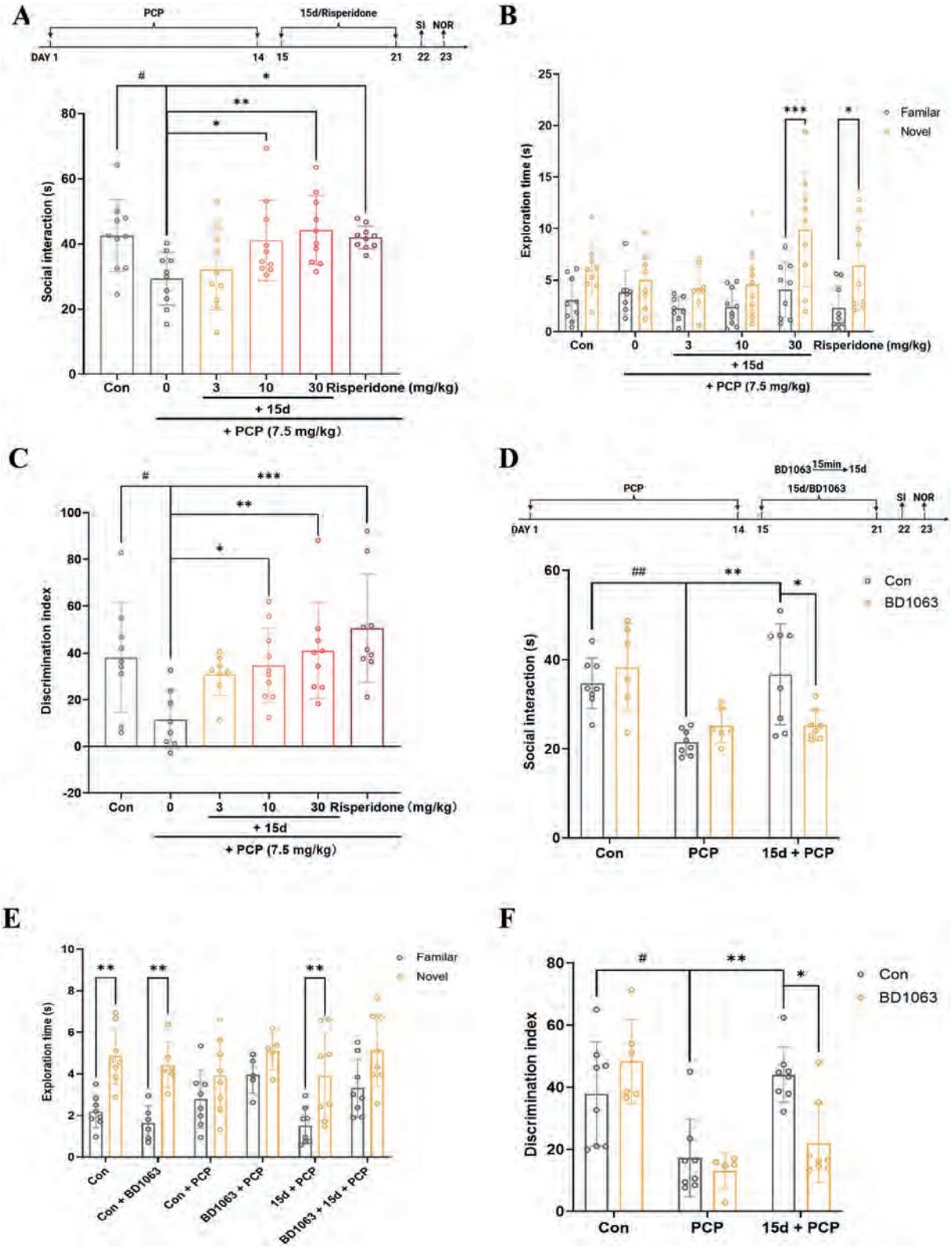

Figure 7 Administration of **15d** improved social deficits and cognitive impairment *via* σ_1R receptor in chronic PCP-treated mice. (A−C) Mice were subcutaneously injected with 7.5 mg/kg PCP for 14 consecutive days to induce social interaction and novel object cognitive impairments[27,28]. The control mice received saline injection. After 14 days of daily PCP administration, **15d**·HCl (3, 10 or 30 mg/kg) or risperidone (1 mg/kg) was then administered orally for 1 week. (A) **15d** significantly attenuated social interaction deficit induced by chronic PCP. (B, C) **15d** significantly attenuated novel object cognitive impairment induced by chronic PCP treatment. The exploration time spent on the novel or the familiar object (B) and the discrimination index (C) are shown. (D−F) Mice were subcutaneously given 0.9% saline or 7.5 mg/kg PCP for 14

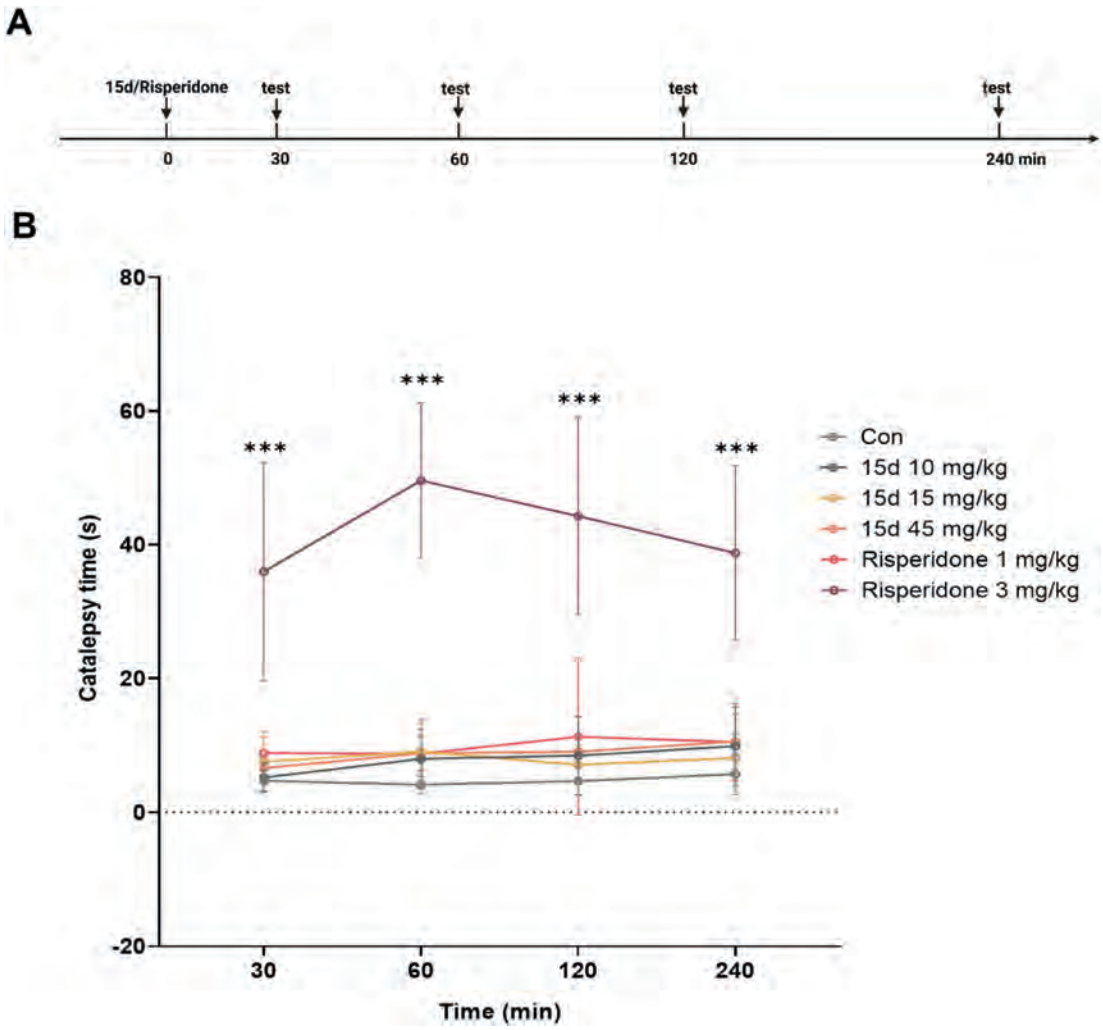

Figure 8 Oral administration of **15d** caused no extrapyramidal adverse reactions at therapeutic doses. (A) Experimental design: **15d** (10, 15, and 45 mg/kg) and risperidone (1 and 3 mg/kg) were administered orally. Catalepsy bar test was subsequently performed as indicated. (B) The effects of **15d** and risperidone on the catalepsy bar test. $n = 8$ animals in each group. The data are shown as the mean ± SD; $n = 8$ mice per group. Statistical analysis was performed by two-way ANOVA; $^{***}P < 0.001$ *vs*. Con. Data are presented as mean ± SEM are provided in Supporting Information Fig. S6.

possessed good selectivity toward σ_1R ($K_i = 1.02$ nmol/L) in relation to σ_2R ($K_i = 199.85$ nmol/L) and 52 other human targets (>1 μmol/L). Moreover, **15d** also showed excellent bioavailability (76.4%) and BBB permeability (B/P ratios: 18.3−46.1), along with low plasma concentrations (70−280.4 ng/mL) at 0.5−4 h, thereby indicating a weak likelihood of peripheral adverse reactions such as cardiovascular or target organ toxicity in toxicology studies. Additionally, **15d** also exhibited nice metabolic and safety profiles. All rendered **15d** as a promising drug candidate.

We further demonstrated that the newly discovered selective σ_1R agonist **15d** effectively improved social withdrawal and cognitive impairment in PCP-induced schizophrenia-like animals, providing the first substantial experimental evidence for the potential of the σ_1R selective agonist for schizophrenia treatment and supporting evidence from previous clinical observations of the beneficial effects of drugs with high affinity for σ_1R[22-24]. Our data not only revealed **15d** as a promising candidate for schizophrenia treatment, but also implied a novel pathway for future antipsychotic drug discovery. Especially, selective σ_1R agonist **15d** exhibited excellent potency in relieving negative symptoms and cognitive defects, both of which remain major clinical challenges in the clinical practice of schizophrenia treatment. Moreover, **15d** exhibited no target-related extrapyramidal effects that are the major adverse effects of dopamine-based antipsychotic drugs. Mechanistically, the activation of σ_1R produces multiple

consecutive days. The control mice (saline treatment) were divided into two groups and received either saline or BD1063 (30 mg/kg, ip) daily. PCP-treated mice were divided into four groups that received daily saline, BD1063, **15d**·HCl (30 mg/kg, *po*) or BD1063 + **15d**·HCl treatment for one week. For **15d**·HCl + BD1063 group, BD1063 was administrated 15 min before **15d**·HCl treatment. After the last dosing, the social interaction test (A) and novel object recognition test (E, F) were performed. The data are shown as mean ± SD. $n = 5-10$ animals in each group. Statistical analysis was performed by two-way ANOVA. $^{*}P < 0.05$, $^{**}P < 0.01$, $^{***}P < 0.001$ compared to Con + PCP. $^{\#}P < 0.05$, $^{\#\#}P < 0.01$ compared to Con. Data are presented as mean ± SEM are provided in Supporting Information Fig. S5.

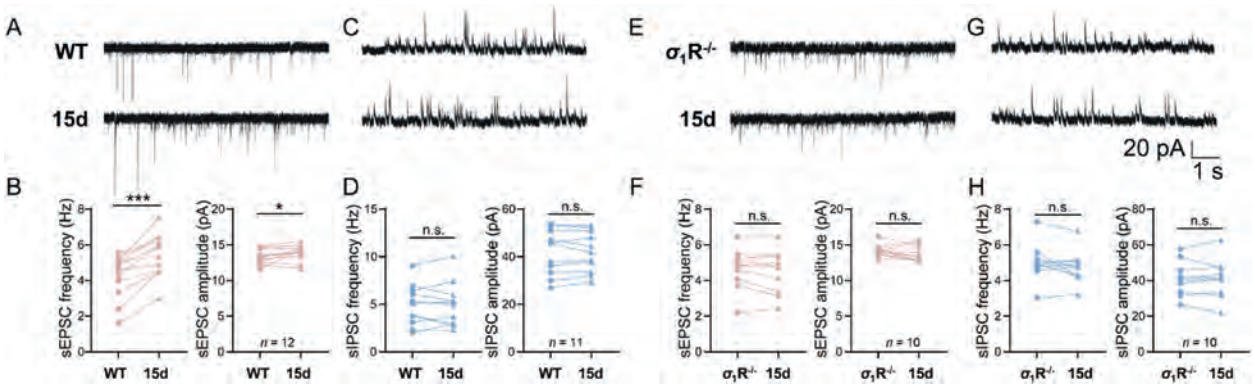

Figure 9 Compound **15d** promotes excitatory synaptic transmission of S1BF L2/3 pyramidal neurons in a σ_1R-dependent manner. The sEPSC and sIPSC pairs were recorded from each cell, in the following order: Ctrl sEPSC, Ctrl sIPSC, **15d** sIPSC, and **15d** sEPSC. (A, C, E, G) Representative traces, and summary graph (B, D, F, H) of the effects of perfusing **15d** (1 μmol/L) on sEPSC or sIPSC frequency and amplitude in adult mice. $n = 10-12$ cells. Statistics are measured *via* paired *t*-test. $^*P < 0.05$, $^{***}P < 0.001$, n.s., not significant.

modulating effects on brain functions. In addition to regulating neuroplasticity[89,90], σ_1R activation has also been shown to elicit neuroprotection and modulate autophagy neuroinflammation[10-16,91-93]. In association with this content, altered expression of brain-derived neurotrophic factor (BDNF) has been well-demonstrated to be associated with the pathophysiology of schizophrenia[94], while σ_1R activation regulating BDNF has been well documented[63,95,96]. We previously reported that the antipsychotic effect of σ_1R allosteric modulator SOMCL668 may attribute to the receptor activation-mediated BDNF production[28]. We here also demonstrated that **15d** treatment stimulated the production of BDNF and levels of phosphor-CREB *in vivo* (Fig. S1E and S1F). BDNF is also known to induce CREB activation, whereas BDNF/CREB regulates neuroplasticity and learning and memory[5,27,95]. It is therefore conceivable that the antipsychotic effect of selective σ_1R agonist **15d** may also involve in the BDNF pathway. In addition to BDNF, σ_1R-regulated GSK3β activity is considered an important mechanism for the receptor function in immunological regulation and neuroprotection, moreover, altered GSK3β activity and its association with the pathological development of schizophrenia are well-established[97-99]. Thus, it is likely both BDNF and GSK3β pathways may contribute to the observed pharmacological effects of **15d**.

Based on the current data, the potential advantages of the use of σ_1R agonists for schizophrenia treatment include the following: (1) Unlike dopamine D_2R-based antipsychotics, there are no target-related EPS or metabolic adverse effects. In fact, σ_1R agonists have been shown to improve Parkinson's motor symptoms and dyskinesia[14,15,91,95,100]. (2) No evidence shows that σ_1R activation has a significant impact on body weight or metabolic profile; (3) Neuroprotection and anti-neuroinflammation of the σ_1R agonist may render it a potential role as a disease modifier. Thus, targeting σ_1R may represent a superior strategy for schizophrenia treatment. It should be noted that potential off-target effects with high doses of **15d** on locomotion and catalepsy cannot completely rule out with the current experimental data. More tests with increasing doses of **15d** should help to clarify this observation.

Additionally, the correlation between the functions of the ligand and σ_1R oligomerization remains obscure, albeit recent X-ray crystallographic studies have unveiled a trimeric form of σ_1R. Given the high affinity and selectivity of **15d**, it may also serve as a valuable pharmacological probe to facilitate our understanding of the mechanisms of σ_1R functional regulation in response to agonist stimulation.

4. Conclusions

By employing structure-based drug design and scaffold repurposing strategy, we identified four analogs, **1a**, **14a**, **15d** and **16d**, as σ_1R selective agonists with excellent binding affinities ($K_i < 4$ nmol/L). Compound **15d** exhibited the best *in vitro* metabolic stability and the lowest intrinsic clearance in liver microsomes. Preliminary druggability assays revealed that compound **15d**, a highly selective σ_1R agonist, had low CYP450 inhibition and inducibility, very good BBB permeability (B/P ratio $= 30-46$), and excellent oral bioavailability ($F = 76.4\%$). Importantly, compound **15d** exhibited potent anti-psychotic efficacy *in vivo*: it significantly attenuated PCP-induced hyperactivity and PPI deficits, implicating the potential against positive symptoms in patients with schizophrenia. Moreover, oral administration of **15d** improved the chronic PCP-induced impairments in social withdrawal and working memory in C57BL/6J mice without extrapyramidal adverse effects, which are the main challenges for current antipsychotic treatments. Mechanistically, **15d** promoted the production of BDNF, inhibited GSK3β and enhanced the excitatory synaptic transmission of pyramidal neurons, which may contribute to its underlined pharmacological effects. Other safety properties such as mini-AMES and DRF toxicology studies of **15d** also revealed no major concerns. Together, our experimental proof-of-concept evidence makes compound **15d** as an excellent candidate for the development of new generation of antipsychotics. Thus, targeting σ_1R may represent a promising novel drug development strategy for schizophrenia.

5. Experimental

5.1. σ_1R radioligand binding assay

The compounds were assayed using Sprague−Dawley (SD) male rat whole-brain homogenates according to a previously reported protocol (more details are provided in the supporting

information)[52]. [^{3}H]-pentazocine, a commonly used probe for the σ_1R receptor, was adopted for monitoring σ_1R binding activity (final concentration: 0.3 nmol/L in the concentration response assays and 0.1−60 nmol/L in the saturation experiments). Radioactivity was measured with a liquid scintillation spectrometer (PerkinElmer). Nonspecific binding of σ_1R was measured in the presence of 10 μmol/L BD1047. The compounds were tested three times in duplicate.

5.2. σ_2R radioligand binding assay

[^{3}H]-1,3-Di(2-tolyl)-guanidine ([^{3}H]-DTG), a commonly used probe for the σ_2R receptor, was adopted for monitoring σ_2R binding activity (final concentration: 10 nmol/L) *via* whole-brain homogenates from SD male rats. Pentazocine (1 μmol/L) was used to block σ_1R binding, and nonspecific binding activity was determined *via* the use of 10 μmol/L haloperidol.

5.3. σ_1R functional assay

We employed multiple assays to detect the agnostic activity of **15d**: (1) The radiolabeled binding assay for σ_1R in the presence of phenytoin (250 μmol/L) was used according to a previously established method[58]. (2) Measurements of the intracellular Ca^{2+} concentration $[Ca^{2+}]_i$ were conducted according to the methods described in the Supporting Information for detailed procedures. (3) To detect the association of σ_1R with Bip, we employed co-immunoprecipitation in HEK293T cells co-transfected with BiP-FLAG along with MYC or SIGMAR1-MYC. Meanwhile, we recently developed a nanoluciferase binary technology (NanoBiT) assay to evaluate the ability of σ_1R to heteromerize with BiP[67] in response to σ_1R agonists in HEK-293-σ_1RLgBiT-BIPSmBiT cells. The methods are described in the Supporting Information

5.4. Liver microsomal stability and cytochrome P450 (CYP450) assay

The liver microsomal stability study and CYP450 inhibition and induction tests of **15d** were conducted by Shanghai ChemPartner Co., Ltd. (Shanghai, China) according to their standard assay protocols.

5.5. Selectivity profiling

The selectivity profile of compound **15d** was assessed at 10 μmol/L in both a 17-panel binding assay of receptors and transporters conducted by Eurofins Cerep (France, Celle L'Evescault) and a 44-panel functional assay of selected human targets performed by ICE Bioscience (Beijing, China), according to their standard assay protocols.

5.6. Mouse pharmacokinetic and brain penetration studies

Studies were performed by Precedo Pharmaceuticals Co., Ltd. (Hefei, China) according to the methods described in the Supporting Information for detailed procedures. Male C57 mice (6−8 weeks, 18−22 g body weight) were purchased from Beijing Vital River Laboratory Animal Technology Co., Ltd. (Beijing, China). Studies were performed with protocols approved by the Institutional Animal Care and Use Committee (IACUC) of Precedo Pharmaceuticals Co., Ltd.

5.7. Behavioral studies

Male C57BL/6 mice, 6−8 weeks old, were acquired from SLAC (Shanghai, China) and housed for a week in the Center of Experimental Animals of Soochow University before the behavioral tests were performed. $\sigma_1R^{-/-}$ KO mice were obtained from the Jackson Laboratory (Bar Harbor, USA) and bred in the same facility. The mouse hyperlocomotion test, prepulse inhibition test, social interaction test, novel object recognition test, and catalepsy bar test were conducted according to our previously published methods[28,30] and are also described in the Supporting Information for detailed procedures. These experiments were double-blinded, and the animals were randomly assigned to different experimental groups. The animal studies were approved (No. 202306A0457) by the animal care and use committees of Soochow University.

5.8. Whole cell recordings

Acute brain slices were prepared as previously described[28,101] from C57BL/6 mice (more details are provided in the Supporting Information). Typically, recordings were made from 2 to 3 cells per brain slice, and 2−3 brain slices per mouse. Whole cell recordings were conducted according to the methods described in the Supporting Information for detailed procedures.

5.9. Statistical analysis

The data from the cellular studies and behavioral studies are expressed as mean ± standard deviation (SD). The mean ± standard error of mean (SEM) for behavioral studies are also attached in the Supporting Information Figs. S4−S6. One-way ANOVA was used for comparisons between multiple groups in one condition, and two-way ANOVA was used for comparisons between multiple groups in two different conditions. Multiple comparative tests of Tukey's and Bonferroni were used for *post hoc* analysis. Statistical significance was set at the 95% confidence level. The statistical tests were performed using GraphPad Prism version 9.0. A value of $P < 0.05$ was considered statistically significant.

5.10. Molecular docking

The cocrystal complexes of 4-IBP interacting with human σ_1R (PDB ID: 5HK2), NE-100 interacting with human σ_1R (PDB ID: 6DK0), and haloperidol interacting with human σ_1R (PDB ID: 6DJZ) were utilized as structural templates for molecular docking studies. First, using the Protein Preparation Wizard module of Schrödinger 9.0, all water molecules were removed from 5HK2, 6DK0 or 6DJZ; broken side chains were repaired; and missing hydrogen atoms were added. The *OPLS2005* force field was then used to assign the protonation states and partial charges. The *Receptor Grid Generation* module was employed to define the binding pocket. The binding pocket, which was 20 Å × 20 Å × 20 Å in size, was positioned directly on the centroid of compound 4-IBP, NE-100 or haloperidol in the σ_1R active site. Next, the rationally designed compounds were pre-processed using the LigPrep mode. Tautomers were generated for each compound at pH = 7.0 ± 2.0 and various combinations of chiralities were produced by setting the maximum number of stereoisomers in Epik to 32. Finally, using the extra precision (XP) scoring function of Glide docking[102], the designed compounds

were docked into the binding pocket of σ_1R. The docking poses and binding affinities were predicted and evaluated.

Acknowledgments

This work was supported by the National Key Research and Development Program of China (2021YFE0206000), National Natural Science Foundation of China (Nos. 22177086, 81973334, and 22477093), STI2030-Major Projects (No. 2021ZD0204004, China), Major Basic Research Project of the Natural Science Foundation of the Jiangsu Higher Education Institutes (No. 22KJA350004, China), and Priority Academic Program Development of the Jiangsu Higher Education Institutes (PAPD). We are very grateful to Prof. Chao Shan (the Wuhan Institute of Virology, Chinese Academy of Sciences) for kindly evaluating the antiviral activity. We thank Prof. Lei Xu at Jiangsu University of Technology for providing the Schrödinger 9.0 simulation package used to construct and validate the molecular docking studies.

Author contributions

Na Ye and Xuechu Zhen conceived and directed the project. Na Ye wrote the manuscript, and Xuechu Zhen revised it. Wanyu Tang, Bang Li, Xiaobao Zhao and Qi Wang conducted the synthesis of compounds and supervised the drug-likeness evaluation experiment; Zhixue Ma, Linghan Gu, Jiaojiao Chen, Shuliu Gao, and Mingmei Wang conducted and supervised animal experiments; Zhexiang Yu, Huicui Yang, Jian Hu, Xing Zou, Guangying Li, and Chaonan Zheng conducted and supervised *in vitro* biology experiments; Sheng Tian, Fan Chen and Na Ye performed the molecular docking; Fan Chen, Wenjing Liu and Yue Li contributed to compounds purification, scale up synthesis, and HPLC analysis; Wenhua Zheng provided experimental technical supports. All authors provided critical feedback and have approved the final version of the manuscript.

Conflicts of interest

The authors declare no conflicts of interest.

Appendix A. Supporting information

Supporting information to this article can be found online at https://doi.org/10.1016/j.apsb.2025.04.028.

References

1. Goldman ML, Pincus HA, Mangurian C. Schizophrenia. *N Engl J Med* 2020;**382**:583−4.
2. Jauhar S, Johnstone M, McKenna PJ. Schizophrenia. *Lancet* 2022; **399**:473−86.
3. Ye N, Wang Q, Li Y, Zhen X. Current emerging therapeutic targets and clinical investigational agents for schizophrenia: challenges and opportunities. *Med Res Rev* 2025;**45**:755−87.
4. Maric NP, Jovicic MJ, Mihaljevic M, Miljevic C. Improving current treatments for schizophrenia. *Drug Dev Res* 2016;**77**:357−67.
5. O'Tuathaigh CMP, Moran PM, Zhen XC, Waddington JL. Translating advances in the molecular basis of schizophrenia into novel cognitive treatment strategies. *Br J Pharmacol* 2017;**174**:3173−90.
6. Granger KT, Sand M, Caswell S, Lizarraga-Valderrama LR, Barnett JH, Moran PM. A new era for schizophrenia drug development — lessons for the future. *Drug Discov Today* 2023;**28**:103603.
7. Kim M, Bezprozvanny I. Structure-based modeling of sigma 1 receptor interactions with ligands and cholesterol and implications for its biological function. *Int J Mol Sci* 2023;**24**:12980.
8. Mishra AK, Mavlyutov T, Singh DR, Biener G, Yang J, Oliver JA, et al. The sigma-1 receptors are present in monomeric and oligomeric forms in living cells in the presence and absence of ligands. *Biochem J* 2015;**466**:263−71.
9. Gromek KA, Suchy FP, Meddaugh HR, Wrobel RL, LaPointe LM, Chu UB, et al. The oligomeric states of the purified sigma-1 receptor are stabilized by ligands. *J Biol Chem* 2014;**289**:20333−44.
10. Ye N, Qin W, Tian S, Xu Q, Wold EA, Zhou J, et al. Small molecules selectively targeting sigma-1 receptor for the treatment of neurological diseases. *J Med Chem* 2020;**63**:15187−217.
11. Ying Z, Ye N, Ma Q, Chen F, Li N, Zhen X. Targeted to neuronal organelles for CNS drug development. *Adv Drug Deliv Rev* 2023; **200**:115025.
12. Sambo DO, Lin M, Owens A, Lebowitz JJ, Richardson B, Jagnarine DA, et al. The sigma-1 receptor modulates methamphetamine dysregulation of dopamine neurotransmission. *Nat Commun* 2017;**8**:2228.
13. Pabba M, Wong AY, Ahlskog N, Hristova E, Biscaro D, Nassrallah W, et al. NMDA receptors are upregulated and trafficked to the plasma membrane after sigma-1 receptor activation in the rat hippocampus. *J Neurosci* 2014;**34**:11325−38.
14. Wang M, Wan C, He T, Han C, Zhu K, Waddington JL, et al. Sigma-1 receptor regulates mitophagy in dopaminergic neurons and contributes to dopaminergic protection. *Neuropharmacology* 2021;**196**: 108360.
15. Guo CH, Cao T, Zheng LT, Waddington JL, Zhen XC. Development and characterization of an inducible Dicer conditional knockout mouse model of Parkinson's disease: validation of the anti-parkinsonian effects of a sigma-1 receptor agonist and dihydromyricetin. *Acta Pharmacol Sin* 2020;**41**:499−507.
16. Jia J, Cheng J, Wang C, Zhen X. Sigma-1 Receptor-modulated neuroinflammation in neurological diseases. *Front Cell Neurosci* 2018;**12**:314.
17. Rafcikova J, Novakova M, Stracina T. Exploring the association between schizophrenia and cardiovascular diseases: insights into the role of sigma 1 receptor. *Physiol Res* 2023;**72**:S113−26.
18. Pabba M, Sibille E. Sigma-1 and *N*-methyl-*d*-aspartate receptors: a partnership with beneficial outcomes. *Mol Neuropsychiatry* 2015;**1**: 47−51.
19. Helmeste DM, Tang SW, Bunney Jr WE, Potkin SG, Jones EG. Decrease in sigma but no increase in striatal dopamine D4 sites in schizophrenic brains. *Eur J Pharmacol* 1996;**314**:R3−5.
20. Weissman AD, Casanova MF, Kleinman JE, London ED, De Souza EB. Selective loss of cerebral cortical sigma, but not PCP binding sites in schizophrenia. *Biol Psychiatry* 1991;**29**:41−54.
21. Watanabe Y, Nunokawa A, Kaneko N, Shibuya M, Egawa J, Someya T. Supportive evidence for the association between the Gln2Pro polymorphism in the SIGMAR1 gene and schizophrenia in the Japanese population: a case-control study and an updated meta-analysis. *Schizophr Res* 2012;**141**:279−80.
22. Albayrak Y, Hashimoto K. Benefical effects of sigma-1 agonist fluvoxamine for tardive dyskinesia and tardive akathisia in patients with schizophrenia: report of three cases. *Psychiatry Investig* 2013;**10**: 417−20.
23. Iyo M, Shirayama Y, Watanabe H, Fujisaki M, Miyatake R, Fukami G, et al. Fluvoxamine as a sigma-1 receptor agonist improved cognitive impairments in a patient with schizophrenia. *Prog Neuropsychopharmacol Biol Psychiatry* 2008;**32**:1072−3.
24. Hayashi T, Su TP. Sigma-1 receptor ligands: potential in the treatment of neuropsychiatric disorders. *CNS Drugs* 2004;**18**:269−84.
25. Mao Q, Zhang B, Tian S, Qin W, Chen J, Huang XP, et al. Structural optimizations and bioevaluation of N−H aporphine analogues as G_q-biased and selective serotonin 5-HT_{2C} receptor agonists. *Bioorg Chem* 2022;**123**:105795.
26. Wang JR, Sun PH, Ren ZX, Meltzer HY, Zhen XC. GSK-3β interacts with dopamine D1 receptor to regulate receptor function: implication

for prefrontal cortical D1 receptor dysfunction in schizophrenia. *CNS Neurosci Ther* 2017;**23**:174−87.
27. Wang P, Cao T, Chen J, Jiang Y, Wang C, Waddington JL, et al. D2 receptor-mediated miRNA-143 expression is associated with the effects of antipsychotic drugs on phencyclidine-induced schizophrenia-related locomotor hyperactivity and with Neuregulin-1 expression in mice. *Neuropharmacology* 2019;**157**:107675.
28. Chen J, Li G, Qin P, Chen J, Ye N, Waddington JL, et al. Allosteric modulation of the sigma-1 receptor elicits antipsychotic-like effects. *Schizophr Bull* 2022;**48**:474−84.
29. Sun H, Zhu L, Yang H, Qian W, Guo L, Zhou S, et al. Asymmetric total synthesis and identification of tetrahydroprotoberberine derivatives as new antipsychotic agents possessing a dopamine D_1, D_2 and serotonin 5-HT_{1A} multi-action profile. *Bioorg Med Chem* 2013;**21**:856−68.
30. Guo Y, Zhang H, Chen X, Cai W, Cheng J, Yang Y, et al. Evaluation of the antipsychotic effect of bi-acetylated l-stepholidine (l-SPD-A), a novel dopamine and serotonin receptor dual ligand. *Schizophr Res* 2009;**115**:41−9.
31. Fallica AN, Pittala V, Modica MN, Salerno L, Romeo G, Marrazzo A, et al. Recent advances in the development of sigma receptor ligands as cytotoxic agents: a medicinal chemistry perspective. *J Med Chem* 2021;**64**:7926−62.
32. Burns M, Guadagnoli N, McCurdy CR. Advances with the discovery and development of novel sigma 1 receptor antagonists for the management of pain. *Expet Opin Drug Discov* 2023;**18**:693−705.
33. Glennon RA. Pharmacophore identification for sigma-1 (sigma1) receptor binding: application of the "deconstruction-reconstruction-elaboration" approach. *Mini Rev Med Chem* 2005;**5**:927−40.
34. Meng F, Xiao Y, Ji Y, Sun Z, Zhou X. An open-like conformation of the sigma-1 receptor reveals its ligand entry pathway. *Nat Commun* 2022;**13**:1267.
35. Schmidt HR, Zheng S, Gurpinar E, Koehl A, Manglik A, Kruse AC. Crystal structure of the human sigma1 receptor. *Nature* 2016;**532**:527−30.
36. Schmidt HR, Betz RM, Dror RO, Kruse AC. Structural basis for sigma1 receptor ligand recognition. *Nat Struct Mol Biol* 2018;**25**:981−7.
37. Baro EL, Catti F, Estarellas C, Ghashghaei O, Lavilla R. Drugs from drugs: new chemical insights into a mature concept. *Drug Discov Today* 2024;**29**:104212.
38. Pushpakom S, Iorio F, Eyers PA, Escott KJ, Hopper S, Wells A, et al. Drug repurposing: progress, challenges and recommendations. *Nat Rev Drug Discov* 2019;**18**:41−58.
39. Tan L, Zhou Q, Yan W, Sun J, Kozikowski AP, Zhao S, et al. Design and synthesis of bitopic 2-phenylcyclopropylmethylamine (PCPMA) derivatives as selective dopamine D3 receptor ligands. *J Med Chem* 2020;**63**:4579−602.
40. Wang P, van der Hoeven D, Ye N, Chen H, Liu Z, Ma X, et al. Scaffold repurposing of fendiline: identification of potent KRAS plasma membrane localization inhibitors. *Eur J Med Chem* 2021;**217**:113381.
41. Tatsumi M, Groshan K, Blakely RD, Richelson E. Pharmacological profile of antidepressants and related compounds at human monoamine transporters. *Eur J Pharmacol* 1997;**340**:249−58.
42. Hashimoto K. Sigma-1 receptors and selective serotonin reuptake inhibitors: clinical implications of their relationship. *Cent Nerv Syst Agents Med Chem* 2009;**9**:197−204.
43. Narita N, Hashimoto K, Tomitaka S, Minabe Y. Interactions of selective serotonin reuptake inhibitors with subtypes of sigma receptors in rat brain. *Eur J Pharmacol* 1996;**307**:117−9.
44. Fotie J, Matherne CM, Mather JB, Wroblewski JE, Johnson K, Boudreaux LG, et al. The fundamental role of oxime and oxime ether moieties in improving the physicochemical and anticancer properties of structurally diverse scaffolds. *Int J Mol Sci* 2023;**24**:16854.
45. Kosmalski T, Kupczyk D, Baumgart S, Paprocka R, Studzinska R. A review of biologically active oxime ethers. *Molecules* 2023;**28**:5041.
46. Cao Z, Yang F, Wang J, Gu Z, Lin S, Wang P, et al. Indirubin derivatives as dual inhibitors targeting cyclin-dependent kinase and histone deacetylase for treating cancer. *J Med Chem* 2021;**64**:15280−96.
47. McGinley MP, Cohen JA. Sphingosine 1-phosphate receptor modulators in multiple sclerosis and other conditions. *Lancet* 2021;**398**:1184−94.
48. Meadows TA, Bhatt DL. Clinical aspects of platelet inhibitors and thrombus formation. *Circ Res* 2007;**100**:1261−75.
49. Micheli F, Cavanni P, Arban R, Benedetti R, Bertani B, Bettati M, et al. 1-(Aryl)-6-[alkoxyalkyl]-3-azabicyclo[3.1.0]hexanes and 6-(aryl)-6-[alkoxyalkyl]-3-azabicyclo[3.1.0]hexanes: a new series of potent and selective triple reuptake inhibitors. *J Med Chem* 2010;**53**:2534−51.
50. Gabrielsen M, Kurczab R, Ravna AW, Kufareva I, Abagyan R, Chilmonczyk Z, et al. Molecular mechanism of serotonin transporter inhibition elucidated by a new flexible docking protocol. *Eur J Med Chem* 2012;**47**:24−37.
51. Coleman JA, Gouaux E. Structural basis for recognition of diverse antidepressants by the human serotonin transporter. *Nat Struct Mol Biol* 2018;**25**:170−5.
52. Guo L, Zhao J, Jin G, Zhao B, Wang G, Zhang A, et al. SKF83959 is a potent allosteric modulator of sigma-1 receptor. *Mol Pharmacol* 2013;**83**:577−86.
53. Diaz JL, Garcia M, Torrens A, Caamano AM, Enjo J, Sicre C, et al. EST64454: a highly soluble $sigma_1$ receptor antagonist clinical candidate for pain management. *J Med Chem* 2020;**63**:14979−88.
54. Cao X, Chen Y, Zhang Y, Lan Y, Zhang J, Xu X, et al. Synthesis and biological evaluation of novel sigma1 receptor ligands for treating neuropathic pain: 6-hydroxypyridazinones. *J Med Chem* 2016;**59**:2942−61.
55. Diaz JL, Christmann U, Fernandez A, Torrens A, Port A, Pascual R, et al. Synthesis and structure-activity relationship study of a new series of selective $sigma_1$ receptor ligands for the treatment of pain: 4-aminotriazoles. *J Med Chem* 2015;**58**:2441−51.
56. Peng Y, Zhang Q, Welsh WJ. Novel sigma 1 receptor antagonists as potential therapeutics for pain management. *J Med Chem* 2021;**64**:890−904.
57. Merlos M, Burgueno J, Portillo-Salido E, Plata-Salaman CR, Vela JM. Pharmacological modulation of the sigma 1 receptor and the treatment of pain. *Adv Exp Med Biol* 2017;**964**:85−107.
58. Cobos EJ, Baeyens JM, Del Pozo E. Phenytoin differentially modulates the affinity of agonist and antagonist ligands for sigma 1 receptors of Guinea pig brain. *Synapse* 2005;**55**:192−5.
59. Dichiara M, Ambrosio FA, Lee SM, Ruiz-Cantero MC, Lombino J, Coricello A, et al. Discovery of AD258 as a sigma receptor ligand with potent antiallodynic activity. *J Med Chem* 2023;**66**:11447−63.
60. Miao Z, Zhong Y, Gan Y, Fu K, Liu W, Cao Z, et al. A novel bifunctional muor agonist and σ_1R antagonist with potent analgesic responses and reduced adverse effects. *J Med Chem* 2023;**66**:16257−75.
61. Gao T, Gao C, Liu Z, Wang Y, Jia X, Tian H, et al. Inhibition of noncanonical Ca^{2+} oscillation/calcineurin/gsk-3β pathway contributes to anti-inflammatory effect of sigma-1 receptor activation. *Neurochem Res* 2022;**47**:264−78.
62. Wang Y, Jiang HF, Ni J, Guo L. Pharmacological stimulation of sigma-1 receptor promotes activation of astrocyte *via* ERK1/2 and GSK3β signaling pathway. *Naunyn-Schmiedebergs Arch Pharmacol* 2019;**392**:801−12.
63. Wang Y, Guo L, Jiang HF, Zheng LT, Zhang A, Zhen XC. Allosteric modulation of sigma-1 receptors elicits rapid antidepressant activity. *CNS Neurosci Ther* 2016;**22**:368−77.
64. Brailoiu GC, Deliu E, Console-Bram LM, Soboloff J, Abood ME, Unterwald EM, et al. Cocaine inhibits store-operated Ca^{2+} entry in brain microvascular endothelial cells: critical role for sigma-1 receptors. *Biochem J* 2016;**473**:1−5.
65. Srivats S, Balasuriya D, Pasche M, Vistal G, Edwardson JM, Taylor CW, et al. Sigma1 receptors inhibit store-operated Ca^{2+} entry

by attenuating coupling of STIM1 to Orai1. *J Cell Biol* 2016;**213**: 65−79.
66. Gasparre G, Abate C, Carlucci R, Berardi F, Cassano G. The sigma$_1$ receptor agonist (+)-pentazocine increases store-operated Ca^{2+} entry in MCF7sigma$_1$ and SK-N-SH cell lines. *Pharmacol Rep* 2017;**69**: 542−5.
67. Morato X, Fernandez-Duenas V, Perez-Villamor P, Valle-Leon M, Vela JM, Merlos M, et al. Development of a novel sigma$_1$ receptor biosensor based on its heterodimerization with binding immunoglobulin protein in living cells. *ACS Chem Neurosci* 2023;**14**: 2201−7.
68. Vitobello A, Mazel B, Lelianova VG, Zangrandi A, Petitto E, Suckling J, et al. ADGRL1 haploinsufficiency causes a variable spectrum of neurodevelopmental disorders in humans and alters synaptic activity and behavior in a mouse model. *Am J Hum Genet* 2022;**109**:1436−57.
69. Li M, He E, Volf N. Time course of the attenuation effect of repeated antipsychotic treatment on prepulse inhibition disruption induced by repeated phencyclidine treatment. *Pharmacol Biochem Behav* 2011; **98**:559−69.
70. Niitsu T, Fujisaki M, Shiina A, Yoshida T, Hasegawa T, Kanahara N, et al. A randomized, double-blind, placebo-controlled trial of fluvoxamine in patients with schizophrenia: a preliminary study. *J Clin Psychopharmacol* 2012;**32**:593−601.
71. Leising J, Barr AM, Procyshyn RM, Ainsworth NJ, White RF, Honer W, et al. High-dose fluvoxamine augmentation to clozapine in treatment-resistant psychosis. *J Clin Psychopharmacol* 2021;**41**: 186−90.
72. Silver H. Fluvoxamine as an adjunctive agent in schizophrenia. *CNS Drug Rev* 2001;**7**:283−304.
73. Zheng W, Xiang YQ, Cai DB, Yang XH, Zhang L, Zheng W, et al. Adjunctive fluvoxamine for schizophrenia: a meta-analysis of randomized double-blind, placebo-controlled trials. *J Clin Psychopharmacol* 2020;**40**:386−90.
74. Breiden B, Sandhoff K. Emerging mechanisms of drug-induced phospholipidosis. *Biol Chem* 2019;**401**:31−46.
75. Lomuscio MC, Abate C, Alberga D, Laghezza A, Corriero N, Colabufo NA, et al. AMALPHI: a machine learning platform for predicting drug-induced phospholipidosis. *Mol Pharm* 2024;**21**: 864−72.
76. Tummino TA, Rezelj VV, Fischer B, Fischer A, O'Meara MJ, Monel B, et al. Drug-induced phospholipidosis confounds drug repurposing for SARS-CoV-2. *Science* 2021;**373**:541−7.
77. Zhen XC, Waddington J. Emerging and evolving concepts in the pathobiology and treatment of psychosis. *CNS Neurosci Ther* 2018; **24**:583−5.
78. Creese I, Burt DR, Snyder SH. Dopamine receptor binding predicts clinical and pharmacological potencies of antischizophrenic drugs. *Science* 1976;**192**:481−3.
79. Chen Z, Fan L, Wang H, Yu J, Lu D, Qi J, et al. Structure-based design of a novel third-generation antipsychotic drug lead with potential antidepressant properties. *Nat Neurosci* 2022;**25**:39−49.
80. Howes OD, Bukala BR, Beck K. Schizophrenia: from neurochemistry to circuits, symptoms and treatments. *Nat Rev Neurol* 2024;**20**: 22−35.
81. Wang YM, Xia CY, Jia HM, He J, Lian WW, Yan Y, et al. Sigma-1 receptor: a potential target for the development of antidepressants. *Neurochem Int* 2022;**159**:105390.
82. Gewirtz GR, Gorman JM, Volavka J, Macaluso J, Gribkoff G, Taylor DP, et al. BMY 14802, a sigma receptor ligand for the treatment of schizophrenia. *Neuropsychopharmacology* 1994;**10**: 37−40.
83. Huber MT, Gotthardt U, Schreiber W, Krieg JC. Efficacy and safety of the sigma receptor ligand EMD 57445 (panamesine) in patients with schizophrenia: an open clinical trial. *Pharmacopsychiatry* 1999; **32**:68−72.
84. Tosh DK, Janowsky A, Eshleman AJ, Warnick E, Gao ZG, Chen Z, et al. Scaffold repurposing of nucleosides (adenosine receptor agonists): enhanced activity at the human dopamine and norepinephrine sodium symporters. *J Med Chem* 2017;**60**:3109−23.
85. Elzahhar PA, Nematalla HA, Al-Koussa H, Abrahamian C, El-Yazbi AF, Bodgi L, et al. Inclusion of nitrofurantoin into the realm of cancer chemotherapy *via* biology-oriented synthesis and drug repurposing. *J Med Chem* 2023;**66**:4565−87.
86. Johnston TH, Geva M, Steiner L, Orbach A, Papapetropoulos S, Savola JM, et al. Pridopidine, a clinic-ready compound, reduces 3,4-dihydroxyphenylalanine-induced dyskinesia in *Parkinsonian macaques*. *Mov Disord* 2019;**34**:708−16.
87. Barthel H, Meyer P, Rullmann M, Becker G, Bronzel M, Marsteller D, et al. Multiple brain effects of pridopidine inhuntington disease patients and healthyvolunteers—a simultaneous sigma-1 receptorPET/MRI study. *J Nucl Med* 2020;**61**:336.
88. Christmann U, Garriga L, Llorente AV, Diaz JL, Pascual R, Bordas M, et al. WLB-87848, a Selective sigma$_1$ receptor agonist, with an unusually positioned NH group as positive ionizable moiety and showing neuroprotective activity. *J Med Chem* 2024;**67**:9150−64.
89. Kourrich S, Su TP, Fujimoto M, Bonci A. The sigma-1 receptor: roles in neuronal plasticity and disease. *Trends Neurosci* 2012;**35**:762−71.
90. Zhang B, Wang L, Chen T, Hong J, Sha S, Wang J, et al. Sigma-1 receptor deficiency reduces GABAergic inhibition in the basolateral amygdala leading to LTD impairment and depressive-like behaviors. *Neuropharmacology* 2017;**116**:387−98.
91. Hong J, Sha S, Zhou L, Wang C, Yin J, Chen L. Sigma-1 receptor deficiency reduces MPTP-induced parkinsonism and death of dopaminergic neurons. *Cell Death Dis* 2015;**6**:e1832.
92. Prasanth MI, Malar DS, Tencomnao T, Brimson JM. The emerging role of the sigma-1 receptor in autophagy: hand-in-hand targets for the treatment of Alzheimer's. *Expert Opin Ther Targets* 2021;**25**: 401−14.
93. Wang JY, Ren P, Cui LY, Duan JY, Chen HL, Zeng ZR, et al. Astrocyte-specific inhibition of sigma-1 receptor leads to depressive-like behaviors in mice *via* activation of NF-kappaB-induced neuroinflammation. *Brain Behav Immun* 2024;**120**:256−74.
94. Liberona A, Jones N, Zuniga K, Garrido V, Zelada MI, Silva H, et al. Brain-derived neurotrophic factor (BDNF) as a predictor of treatment response in schizophrenia and bipolar disorder: a systematic review. *Int J Mol Sci* 2024;**25**:11204.
95. Hashimoto K. Sigma-1 receptor chaperone and brain-derived neurotrophic factor: emerging links between cardiovascular disease and depression. *Prog Neurobiol* 2013;**100**:15−29.
96. Fukunaga K, Moriguchi S. Stimulation of the sigma-1 receptor and the effects on neurogenesis and depressive behaviors in mice. *Adv Exp Med Biol* 2017;**964**:201−11.
97. Weng YT, Chien T, Kuan II, Chern Y. The TRAX, DISC1, and GSK3 complex in mental disorders and therapeutic interventions. *J Biomed Sci* 2018;**25**:71.
98. Albeely AM, Williams OOF, Perreault ML. GSK-3β disrupts neuronal oscillatory function to inhibit learning and memory in male rats. *Cell Mol Neurobiol* 2022;**42**:1341−53.
99. Petrikis P, Polyzou A, Premeti K, Roumelioti A, Karampas A, Georgiou G, et al. GSK3β and mTORC1 represent 2 distinct signaling markers in peripheral blood mononuclear cells of drug-naive, first episode of psychosis patients. *Schizophr Bull* 2022;**48**: 1136−44.
100. Francardo V, Bez F, Wieloch T, Nissbrandt H, Ruscher K, Cenci MA. Pharmacological stimulation of sigma-1 receptors has neurorestorative effects in experimental parkinsonism. *Brain* 2014;**137**: 1998−2014.
101. Li MY, Miao WY, Wu QZ, He SJ, Yan G, Yang Y, et al. A critical role of presynaptic cadherin/catenin/p140Cap complexes in stabilizing spines and functional synapses in the neocortex. *Neuron* 2017; **94**:1155−11572 e8.
102. Friesner RA, Banks JL, Murphy RB, Halgren TA, Klicic JJ, Mainz DT, et al. Glide: a new approach for rapid, accurate docking and scoring. 1. Method and assessment of docking accuracy. *J Med Chem* 2004;**47**:1739−49.